

**REMOVAL OF METAL IONS FROM INDUSTRIAL EFFLUENTS  
AND ACID MINE DRAINAGE BY  
METAL SULPHIDE PRECIPITATION**

Report to the  
Water Research Commission

by

**Moses Nduna and Alison Lewis**

Crystallization and Precipitation Research Unit  
Department of Chemical Engineering  
University of Cape Town

**WRC Report No. 2108/1/14  
ISBN 978-1-4312-0588-2**

**September 2014**

**Obtainable from**

Water Research Commission  
Private Bag X03  
Gezina, 0031

[orders@wrc.org.za](mailto:orders@wrc.org.za) or download from [www.wrc.org.za](http://www.wrc.org.za)

**DISCLAIMER**

This report has been reviewed by the Water Research Commission (WRC) and approved for publication. Approval does not signify that the contents necessarily reflect the views and policies of the WRC, nor does mention of trade names or commercial products constitute endorsement or recommendation for use.

## EXECUTIVE SUMMARY

The purpose of this research was to further the understanding of metal sulphide precipitation in the treatment of acid mine drainage and metal ion impregnated industrial wastewater. During the process of metal sulphide precipitation the physico-chemical properties of the precipitant material had a significant effect on the overall viability of the metal removal process. The aim of the work was to ascertain the conditions necessary for optimal metal ion removal and this was achieved by addressing the following objectives:

1. Characterisation of the effect of operating conditions on the physical properties of the formed metal sulphide precipitate.
2. Investigation of properties that affected the solid-liquid separation characteristics of formed particles.
3. Investigation of factors with potential influence on the solid-liquid separation characteristics of formed particles.

In line with objective 1, the current work showed that the contacting conditions with respect to the metal-sulphide ratio had a significant effect on the physical properties of the precipitant material. An excess amount of sulphide during contacting led to a stable colloidal suspension due to the highly negative zeta potential of the resultant particles. Although this effect was observed in both the copper and zinc sulphide systems, it occurred to a greater extent in the copper sulphide system. This resulted in substantially more negatively charged particles of CuS than ZnS under similar conditions of precipitation. Further work also suggested that metal sulphide particle aggregation was inhibited above a certain threshold value of zeta potential and this threshold value was metal sulphide specific. Consequently a correlation was developed between settling characteristics and zeta potential. Particles with a large zeta potential magnitude formed more stable colloidal suspensions whilst particles with a small zeta potential magnitude did not form stable suspensions.

Conventional surface modifying techniques, post-precipitation, were used to induce changes in the zeta potential of precipitant particles in-order to investigate the subsequent solid-liquid separation characteristics. The three surface-modifying techniques studied were: effect of suspension pH, addition of sulphide, and addition of cations. All three factors were found to have a considerable effect on particle zeta potential and subsequent coagulation properties, although this was to varying extents.

The investigation of factors that potentially influenced solid-liquid separation led to the use of non-conventional particle surface modifying techniques. Post-precipitation, the partial oxidation of precipitant material was investigated with the aim of reducing the particle zeta potential in-order to increase aggregation and consequently settling. This was found to have a considerable effect on improving settling while maintaining a high metal ion recovery. In addition to this, precipitation under controlled supersaturation was also investigated. This was achieved by using solid FeS as a sulphide source via dissolution. The process was mass-transfer limited and this was exploited as a control mechanism for sulphide dosing. Although supersaturation was found to be significantly reduced, the process was not viable due to encapsulation of the FeS particles by the precipitating pollutant metal ions.

**In summary, metal sulphide precipitation has shown potential as a method for the removal of metals from industrial pollutant streams. Although its relatively low solubility products and fast reaction kinetics mean that the process has a number of challenges, it is still a superior choice to that of metal hydroxide precipitation.**

The findings of the current work are, firstly, that that metal sulphide particles obey the DLVO theory. However, the reported threshold value for the promotion of aggregation of about -38 mV is difficult to achieve under viable operational conditions. The pH during precipitation either has to be very high, resulting in the need for a high dosage of pH modifiers, or the colloidal suspension has to be treated with significant amounts of coagulants. This reduces the viability of sulphide precipitation as a precipitation method.

This work has also shown that other mechanisms of inducing settling, such as partial oxidation of precipitant material, are effective, but only in synthetic mono-component streams. The consequence of using such a technique for typical industrial multicomponent streams and acid mine drainage is that altering the solution redox not only affects the target material, but may induce catalytic reactions that may transform the precipitant material into an undesired product. Further studies with multicomponent systems would be required.

The last major finding of this work is that using FeS as a slow sulphide release source for the precipitation of lower solubility product metal sulphides suffers from limitations that render it not viable for industrial use. The encapsulation of FeS by ZnS that was observed in the current process inhibited further dissolution of the sulphide source, thus stopping the precipitation process.

It is recommended that future work in this area focus on the production of a metal sulphide product that is easily separable from the industrial waste stream. Two of the most promising contenders for processes are **electrocoagulation** and **magnetic field** application. Both of these processes have the ability to address the biggest issue with metal sulphide formation – the difficulty of promoting settling - and both of them do so without the addition of any additional reagents.

## ACKNOWLEDGEMENTS

The writers wish to express their gratitude:

To the staff of the Crystallization and Precipitation Unit and the Mechanical Workshop, in the Chemical Engineering Department at the University of Cape Town for their contribution to the research reported here;

To the Water Research Commission (WRC) for the funding support;

To the members of the Reference Group for their contributions to and guidance of the project, namely: Dr JE Burgess (WRC), Mr A Wurster (Independent consultant), Dr NE Ristow (Interwaste), Ms R Mühlbauer (Anglo American), Mr JS Beukes (Coaltech), Prof LF Petrik (University of the Western Cape), Mr IW van der Merwe (Proxa Pty Ltd), Mr P Günther (Anglo American), Prof N Torto (Rhodes University), Mr D Howard (TWP Projects Pty Ltd), Mr S Hareeparsad (Sasol Technology), Dr G Madzivire (University of the Western Cape), and Mr HM du Plessis (Independent consultant).



# TABLE OF CONTENTS

<b>EXECUTIVE SUMMARY</b>	<b>i</b>
<b>ACKNOWLEDGEMENTS</b>	<b>iii</b>
<b>TABLE OF FIGURES</b>	<b>vii</b>
<b>TABLE OF TABLES</b>	<b>vii</b>
<b>NOMENCLATURE</b>	<b>viii</b>
<b>GREEK SYMBOLS</b>	<b>viii</b>
<b>1 Introduction</b>	<b>1</b>
<b>2 Objectives</b>	<b>2</b>
<b>3 Theory</b>	<b>3</b>
3.1 Introduction to precipitation	3
3.2 Supersaturation	3
3.3 Particle rate processes	3
3.4 Nucleation	4
3.5 Aggregation	4
3.6 Surface Charge	5
3.7 Electrical Double Layer	5
3.8 Ion Distribution in the Double Layer	6
3.9 Colloidal Stability	8
3.10 Electrophoresis	10
3.11 Particle size distribution analysis technique	10
<b>4 Literature Review</b>	<b>12</b>
<b>5 Experimental Studies</b>	<b>15</b>
5.1 Analytical Methods	15
5.1.1 Zeta potential measurements	15
5.1.2 pH measurements	15
5.1.3 Sulphide analysis	15
<b>6 Studies to investigate effect of reaction conditions on particle characteristics</b>	<b>16</b>
6.1 Objective	16
6.2 Materials and methods	16
6.2.1 Reagents	16
6.2.2 Experimental setup	16
6.2.3 Experimental Procedure	17
6.3 Results and Discussion	17
6.4 Conclusions	18
<b>7 Studies to investigate whether or not there is a specific zeta potential value at which aggregation is suppressed</b>	<b>19</b>
7.1 Objective	19
7.2 Materials and methods	19
7.2.1 Experimental procedure	19
7.3 Results and Discussion	19
7.4 Conclusions	20
<b>8 Effect of post-precipitation conditions on surface properties of colloidal metal sulphide particles</b>	<b>21</b>
8.1 Materials and Methods	21
8.1.1 Experimental set up	21
8.1.2 Experimental procedure	21
8.1.3 Metal Precipitation	22

8.1.4	Surface studies	22
8.2	Results and discussion	22
8.2.1	Effect of pH on surface properties	22
8.2.2	Effect of sulphide addition on surface properties	26
8.2.3	Effect of cation addition on surface properties	27
8.3	Conclusions	28
<b>9</b>	<b>Potential factors affecting solid-liquid separation</b>	<b>30</b>
9.1	Background and objective	30
9.2	Materials and Methods	31
9.2.1	Reagents	31
9.2.2	Experimental Design	31
9.2.3	Experimental Procedure	32
9.2.4	Sampling and analytical methods	32
9.3	Results	32
9.4	Discussion	34
9.5	Conclusions	35
<b>10</b>	<b>Investigation of using FeS Slurry as a slow release sulphide source</b>	<b>36</b>
10.1	Background	36
10.1.1	Choice of precipitating agent	37
10.1.2	Operating conditions	38
10.2	Scope of investigation	39
10.3	Materials and Methods	39
10.3.1	Experimental Design	39
10.3.2	Reagents	39
10.3.3	Experimental set-up	39
10.3.4	Analytical Techniques	40
10.4	Experimental Procedures	40
10.4.1	Precipitation of FeS	40
10.4.2	Investigation of FeS dissolution	41
10.4.3	Precipitation of pollutant metal ions	41
10.5	Results	41
10.6	Discussion	44
10.7	Supersaturation reduction	44
10.8	Conclusions	45
<b>11</b>	<b>Overall conclusions</b>	<b>46</b>
11.1	Studies to investigate effect of reaction conditions on particle characteristics	46
11.2	Studies to investigate whether or not there is a specific zeta potential value at which aggregation is suppressed	46
11.3	Potential factors affecting solid-liquid separation	46
11.4	Investigation of using FeS Slurry as a slow release sulphide source	47
<b>12</b>	<b>References</b>	<b>49</b>

## TABLE OF FIGURES

Figure 3.1: Nucleation mechanisms (Mullin, 2001) .....	4
Figure 3.2: Electrical double layer according to Helmholtz model, different spheres represent different charges (Everett, 1988).....	6
Figure 3.3: Diffuse electrical double layer with thermal motion (Everett, 1988) .....	6
Figure 3.4: Charge potential with distance from particle surface (Hunter, 1986) .....	7
Figure 3.5: Representation of the diffuse double layer (after Mehta et al., 2011).....	8
Figure 3.6: The net interaction energy between two colliding particles (Hunter, 1986) .....	10
Figure 4.1: Change in zeta potential of metal sulphide as a function of metal to sulphide ratio at pH6 (Mokone et al., 2010) .....	13
Figure 4.2: Change in the $m_2$ (related to surface area) for metal sulphide precipitates with different metal to sulphide ratios (Mokone et al., 2010).....	13
Figure 6.1: Experimental setup for the precipitation of metal sulphide particles .....	16
Figure 6.2: Change in zeta potential of metal sulphide particles as a function of metal:sulphide molar ratio at pH 6 compared with Mokone et al. (2010).....	17
Figure 6.3: Change in zeta potential of metal sulphide particles as a function of metal:sulphide ratio .....	18
Figure 7.1: Zeta potential values at which aggregation is inhibited .....	20
Figure 8.1: Semi batch experimental set-up for the precipitation of metal sulphide particles .....	21
Figure 8.2: Change in zeta potential as a function of pH for CuS and ZnS.....	23
Figure 8.3: Change in $m_2$ and number based mean of CuS particles with pH .....	24
Figure 8.4: Change in $m_2$ and number based mean of ZnS particles with pH.....	25
Figure 8.5: Change in zeta potential with sulphide concentration.....	26
Figure 8.6: Change in zeta potential with cation addition .....	27
Figure 9.1: Surface structure of sulphides and oxides (Bebie et al., 1997) .....	30
Figure 9.2: Effect of oxidation on zeta potential of CuS .....	33
Figure 9.3: Change in zeta potential of CuS with pH .....	33
Figure 9.4: Effect of oxidation on zeta potential of ZnS particles .....	34
Figure 10.1: pH dependence of hydrogen sulphide speciation (Lewis, 2010).....	37
Figure 10.2: MeS solids percentage versus pH at 25°C obtained from Visual minteq.....	39
Figure 10.3: Batch reactor used for the precipitation of FeS .....	40
Figure 10.4: Effect of pH on the concentration of ferrous ions in solution with time.....	42
Figure 10.5: Variation of $Fe^{2+}$ ion concentration with time during simultaneous dissolution of FeS and precipitation of ZnS.....	43
Figure 10.6: Concentration of $Zn^{2+}$ ions in solution during dissolution of FeS.....	43
Figure 10.7: Comparison between the Conventional Supersaturation Level and the Supersaturation Levels Achieved Through the Use of FeS .....	45

## TABLE OF TABLES

Table 9.1: IEP of selected metal sulphides .....	31
Table 10.1: Metal sulphide equilibrium $k_{sp}$ values at 18°C (Schlauch, 1978).....	38

## NOMENCLATURE

$a$	activity ( $\text{mol}/\text{dm}^3$ )
$A$	sphere particle radius (m)
$a^*$	activity at equilibrium ( $\text{mol}/\text{dm}^3$ )
$A_H$	Hamaker constant (J)
$C$	concentration ( $\text{mol}/\text{dm}^3$ )
$c$	number of ions per $\text{m}^3$
$D$	dielectric constant
$e$	elementary charge (C)
$E$	electric field (V/m)
$G$	Gibbs energy (J)
$H$	shortest distance between two stern layers (m)
$k$	boltzmann's constant (J/molecule.K)
$k_d$	mass transfer coefficient
$k_r$	reaction rate constant
$K_{sp}$	solubility product
$\dot{m}$	mass flux ( $\text{kg}/\text{m}^2.\text{s}$ )
$N_A$	Avogadro's constant ( $\text{mol}^{-1}$ )
$pH_{iep}$	isoelectric point
$R$	universal gas constant (J/mol.K)
$S$	supersaturation
$T$	temperature (kelvin)
$V_R, V_A$	interaction energy, repulsion and attraction
$z$	valence
$\kappa a$	ratio (radius of curvature to double layer thickness for a particle)
$\kappa$	inverse Debye length ( $\text{m}^{-1}$ )

## GREEK SYMBOLS

$\rho$	net charge density ( $\text{C}/\text{m}^3$ )
$\sigma$	surface area ( $\text{m}^2$ )
$\psi$	electrical potential (V)
$\gamma$	interfacial energy (J)
$\zeta$	zeta potential (V)
$\eta$	viscosity (Pa/s)
$\epsilon$	permittivity of medium
$\mu$	chemical potential (J/mol)
$\mu_E$	electrophoretic mobility ( $\text{m}^2.\text{V}.\text{s}$ )
$v_L$	electrophoretic velocity (m/s)

## 1. Introduction

The removal of metal ions from industrial effluents by sulphide precipitation is a well-known process characterised by potentially high removal efficiency and selective metal precipitation over a broad pH range. However, the widespread application of this treatment technology has previously been limited due to the use of expensive chemicals and the accompanying production of toxic hydrogen sulphide gas, particularly when treating acidic effluents.

In recent years, novel biological processes, based on the activity of sulphate reducing bacteria (SRB) for safe and cost effective reduction of sulphates to sulphide have been introduced. These processes are accompanied by metal removal as metal sulphide precipitates. However, a number of challenges exist around the precipitation step, particularly where the removal and recovery of metals is concerned.

Due to the low solubility of metal sulphides and the high affinity between the reactants, the metal sulphide precipitation reactions are inherently driven by extremely high supersaturations. The resulting precipitation reaction is difficult to control and a large number of submicron particles are formed during the process. Thus, solid-liquid separation and subsequent recovery become a significant technical challenge and, despite the low solubility and theoretically high efficiency of metal sulphide precipitation processes, the practical efficiency is often significantly lower.

This project proposes to focus on elucidating the mechanisms involved in the formation of metal sulphide precipitates under different operating conditions. Although several studies have been conducted on precipitation of metal sulphides from solution (Bryson and Bijsterveld, 1991; Mishra and Das, 1992; Rickard, 1995; Harmandas and Koutsoukos, 1996; Veeken et al., 2003; van Hille et al., 2005; Bijmans et al., 2009; Sampaio et al., 2010), the physico-chemical processes of nucleation and crystal growth processes involved in the precipitation of metals as sulphides remain uncertain.

Therefore, the objective of this research is to develop an understanding of the processes involved in metal sulphide precipitation and thus why some sulphide precipitates are less amenable to separation than others. To this end the underlying physico-chemical mechanisms involved in the precipitation of various metal sulphides, as well as sulphide speciation, charge development, and effects of oxidation will be investigated. The primary sulphides chosen for this study were CuS and ZnS because the respective cations are predominantly the most abundant metal ions in acid mine drainage after iron, and they represent opposite spectrums in terms of solubility of metal sulphides. Although FeS is abundant in acid mine drainage, it was not chosen because it has a very different behaviour to other transition metal sulphides. However, other metal sulphides may also be subject to the investigation depending on the specific scope of the evolving objectives.

## 2. Objectives

The purpose of the research was to further the understanding of the precipitation of metal sulphides in the treatment of acid mine drainage via sulphate reduction and metal precipitation.

1. The first aim was to characterise the effect of operating conditions on the physical characteristics of the formed metal sulphide precipitate. This aim was divided into three objectives:

a. To investigate the effect of metal to sulphide ratio on precipitation behaviour. In classical industrial crystallization approaches, the metal to sulphide ratio is not considered specifically, as this parameter is incorporated in the measurement of supersaturation. However, it is apparent that the exact proportions of metal to sulphide play an important role in the final characteristics of the formed precipitates. The effect of metal:sulphide ratio on the precipitation process at a constant operational pH was investigated. These studies were carried out on a number of model metal systems.

b. To investigate the effect of the operating pH on the precipitation process. The precipitation process will be operated at different pH levels while keeping the metal to sulphide ratio constant. These studies will be carried out on a number of model metal systems.

c. To infer the mechanisms involved in particle formation, using a technique based on moment transformations of the number density function  $n(L)$  described by Randolph and Larson (1988). This technique has been successfully used by Bramley and Hounslow (1996), Ntuli and Lewis (2007), and Hove et al (2008) but has not yet been applied to metal sulphide precipitation.

2. The second aim is to investigate the factors affecting the solid-liquid separation characteristics of the formed particles. The effects of the processing conditions on solid-liquid separation characteristics of the formed precipitates will be quantified using particle size distribution measurements, settling characteristics and zeta potential measurements for surface charge determination. These studies will be carried out on a number of model metal systems.

3. The third aim is to investigate factors that potentially influence the solid-liquid separation characteristics of the formed particles.

As a result of the investigations carried out in aim (2), it should be possible to identify a number of factors, possibly different additives that would influence the separation characteristics of the formed precipitates. For example, the divalent and trivalent ions most commonly found in metal contaminated wastewater, e.g. Ca, Al, Mg and Na have been found to play a key role in granulation phenomena (Pevere et al., 2007). Thus the effect of these ions (as well as other additives) on coagulation and aggregation phenomenon will be quantified by measuring their effect on particle size distribution, surface charge and settling characteristics of the precipitate.

### 3. Theory

#### 3.1. Introduction to precipitation

Precipitation refers to a generally fast crystallisation process characterised by the formation of a sparingly soluble solid phase (Söhnel and Garside, 1992). The solid phase is generally brought about by a fast chemical reaction. Due to fast reaction kinetics and the sparingly soluble nature of most precipitating compounds, precipitation processes are characterised by high levels of supersaturation, high nucleation rates and production of a large number of particles (i.e.  $> 10^{11}$  particles per  $m^3$ ) with a small particle size (i.e.  $< 10 \mu m$ ) (Söhnel and Garside, 1992).

Precipitation in its various forms and configurations has been used in the scavenging of dissolved metal ions from industrial waste water and acid mine drainage. The properties (i.e. particle size, morphology and surface area) of formed precipitates are vital in most practical applications and can have major impact on post-precipitation processing, such as solid-liquid separation (Söhnel and Garside, 1992). Metal sulphide precipitation involves the reaction of sulphide ions with metal ions to give an insoluble metal sulphide species.

#### 3.2. Supersaturation

Supersaturation is defined as the thermodynamic driving force behind all precipitation processes. Söhnel and Garside (1992) state that the extent of precipitation in a precipitating system governs the particle rate processes, such as nucleation, growth and aggregation. Mersmann (2001), describes supersaturation as the difference between the chemical potential of the solute in solution,  $\mu$ , and the chemical potential of the solution in equilibrium with the solid phase,  $\mu^*$ . The change in chemical potential,  $\Delta\mu$ , is defined by the following relation, Equation 1.

$$\Delta\mu = nRT \ln\left(\frac{a}{a^*}\right) \quad 1$$

Where  $a$  is the activity of the reacting species in solution and  $a^*$  is the ionic activity of the reacting species at equilibrium

According to Mersmann (2001), supersaturation in aqueous solutions expressed in ion activity is given as shown by Equation 2:

$$S = \left(\frac{(C_A)^x (C_B)^y}{K_{sp}}\right)^{\frac{1}{x+y}} \quad 2$$

Where  $K_{sp} = (C_A^*)^x (C_B^*)^y$  and  $C_A$  and  $C_B$  are ion concentrations of the reacting species and (\*) denotes conditions at equilibrium. Equation 1 and 2 (Mersmann, 1999)

#### 3.3. Particle rate processes

Kinetic processes of nucleation, growth, aggregation and breakage can be defined as particle rate processes and are responsible for the change in particle size distribution with time during precipitation.

### 3.4. Nucleation

The formation of the first thermodynamically stable solid (nuclei) in solution can be defined as nucleation (Söhnel and Garside, 1992). The driving force for the creation of nuclei is the decrease in the chemical potential of molecules leaving the solution due to a decrease in the Gibbs free energy between the two bulk phases. Various mechanisms are responsible for nucleation and these are schematically represented in Figure 3.1.

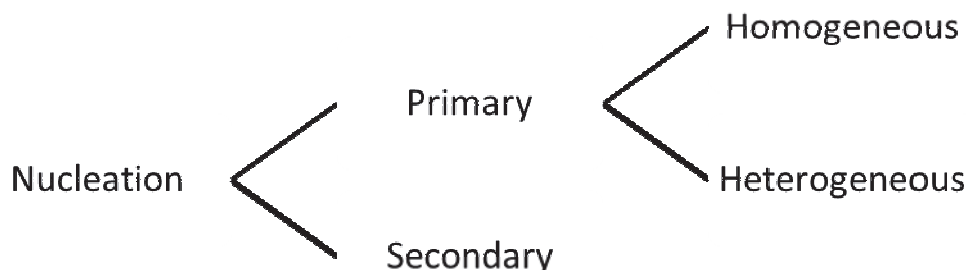


**Figure 3.1: Nucleation mechanisms (Mullin, 2001)**

Primary nucleation is the formation of a new solid phase, not influenced by an existing solid phase. There are two types of primary nucleation: homogenous nucleation, which results in the formation of a solid phase not initiated by the presence of any solid, and heterogeneous nucleation, which results in the formation of a solid phase catalysed by the presence of a foreign solid phase (Mullin, 2001). Secondary nucleation refers to the birth of nuclei at the interface of the crystallising material. This type of nucleation is very rare during precipitation of sparingly soluble compounds (Söhnel and Garside, 1992).

### 3.5. Aggregation

Aggregation occurs when particles collide and adhere to one another to form larger particles (Söhnel and Garside, 1992). Franke and Mersmann (1995) stated that aggregation consists of three steps:

- i. The collision of particles.
- ii. The staying together of particles.
- iii. The cementing of particles by formation of crystalline bridges between particles.

Particles can collide as a result of various transport mechanisms that include Brownian motion and mechanical stirring. Two colliding particles experience both repulsion and attraction to varying degrees, and the nature of the overall particle interactions depends on the larger of the two forces. The magnitude of repulsion and attraction experienced by colliding particles depends on particle surface characteristics (i.e. surface charge) and solution chemistry. Particles in an unstable solution brought together by Brownian motion undergo perikinetic aggregation, while those brought together by mechanical stirring undergo orthokinetic aggregation. The rate of aggregation in a colloid system may be defined in terms of suspension stability. A solution is termed stable if the majority of dispersed particles collide without consequence and unstable if particle collisions lead to the formation of new larger particles. Stable solutions tend to evolve with time as numerous smaller particles collide to form fewer large particles. Aggregation is a surface mediated reaction and

therefore it is highly dependent on surface properties, such as surface charge of the primary particles.

### 3.6. Surface Charge

A surface or interface exists where there is an abrupt change in system properties with distance. Typical properties that exhibit an abrupt change at an interface are “crystal structure, crystal orientation, chemical composition, density and ferromagnetic or paramagnetic ordering” (Hudson, 1998). Colloidal surfaces may develop charge as a result of one or more of the following mechanisms.

i. If in contact with a different phase, charge may arise due to a difference in electron/ion affinity of the two phases.

ii. Ionisation of surface groups:

In cases where the surface contains acidic groups their dissociation gives rise to a negatively charged surface, and conversely a basic surface takes on a positive charge. The magnitude of the surface charge depends on the extent of dissociation,  $K_a$  or  $K_b$  of the respective acid or basic surface. Ionisation of surface groups can be inhibited to zero (Point of Zero Charge, PZC) by (a) decreasing pH in case of an acid surface and (b) increasing pH in case of a basic surface.

iii. Isomorphous substitution:

This can be the exchange of an adsorbed, intercalated, or structural ion with one of a lower valency, resulting in a negatively charged surface.

iv. Colloid surface defects:

This results from surface bond cleavage/unsatisfied bonds.

v. Differential solution of ions from the surface of a sparingly soluble crystal/colloid. This can be explained by an example of a silver iodide crystal placed in water, solution occurs until the ionic product equals the solubility product  $[Ag^+][I^-]=K_s=10^{-16} \text{ (mol dm}^{-3}\text{)}^2$ . In the event that an equal amount of ions  $[Ag^+] = [I^-] = 10^{-8} \text{ mol dm}^{-3}$  dissolve, the surface of the remaining crystal will remain uncharged. Silver ions preferentially dissolve leaving a negatively charged surface, a result of iodine ions in slight excess (Hunter, 1986; Everett, 1988).

### 3.7. Electrical Double Layer

When a charged colloidal particle is immersed in an electrolyte solution it is surrounded by ions of the opposite sign to balance the surface charge. Applied to the electrostatic case, Boltzmann's law indicates that if at some point in an electrolyte solution a charge potential exists,  $\psi$ , the region around that point will have a concentration of ions defined by (Everett, 1988):

For positive ions

$$c(+) = c^0 \exp(-z_+ e \psi / kT) \quad 3$$

where  $z_+$  is the valence of the positive ion,  $c^0$  the concentration of positive ions in a region where  $\psi=0$  and  $e$  the elementary/protonic charge.

For negative ions

$$c(-) = c^0 \exp(+z_-.e\psi/kT) \quad 4$$

In this region around the charge centre, an electrical imbalance of charges exists, which in the case of  $z_+ = z_- = 1$  is

$$c(+) - c(-) = c^0 [\exp(-e\psi/kT) - \exp(e\psi/kT)] \quad 5$$

If the region under consideration is close to a negatively charged centre,  $\psi$  will be negative and  $[c(+) - c(-)]$  will be positive. Consequently, around a negative ion there will be an excess of positive charge, called a charge cloud or ionic atmosphere. The electrolyte solution as a whole, however, remains electrically neutral and it is the charge cloud or ionic atmosphere that is called the electrical double layer.

### 3.8. Ion Distribution in the Double Layer

It is important to understand the nature, composition and arrangement of the counter-ions in the electrical double layer. Yang-Xin and co-workers (2004) stated that the stability of a charge stabilized colloidal dispersion depends on the distribution and composition of small ions in the electrical double layer. Various models attempt to address this, but the simplest model of the double layer is attributed to Helmholtz, in which he envisaged an arrangement of charges in two rigid parallel planes as shown in Figure 3.2 (Everett, 1988)

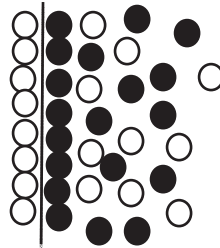


**Figure 3.2: Electrical Double layer according to Helmholtz model, different spheres represent different charges (Everett, 1988)**

The Helmholtz model has however been recognised as an inadequate representation of the double layer because of its inability to account for thermal motion. Counter-ions become spread out in space as a result of thermal motion to form a diffuse double layer, in which the local ion concentration is determined by equation (5). Further attempts to understand the nature of the double layer led to the development of the Gouy (1910) and Chapman (1913) theory (Hiemstra et al., 1989).

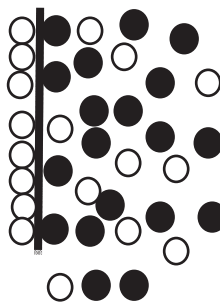


**Figure 3.3: Diffuse electrical double layer with thermal motion (Everett, 1988)**

Gouy-Chapman model states that the counter-ions are not rigidly held around the colloid surface, but diffuse into the bulk phase until the counter potential set up by their departure inhibits such movement. A diagram showing the electrical double layer as envisaged by Gouy and Chapman is shown Figure 3.3 (Everett, 1988). In the case of a plane surface with a uniformly distributed charge, the charge density in solution falls exponentially with distance from the surface as shown Figure 3.4, at distance  $1/\lambda$  the potential drops by a factor of  $1/e$  as shown in Equation 6,

$$\Psi = \psi^0 \exp(-x/\lambda) \quad 6$$

This measurement can be used to measure the width of the double layer and according to theoretical equations it may assume the value defined by Equation 7:

$$1/\lambda = [\epsilon k T / e^2 \sum c_i z_i^2]^{0.5} \quad 7$$

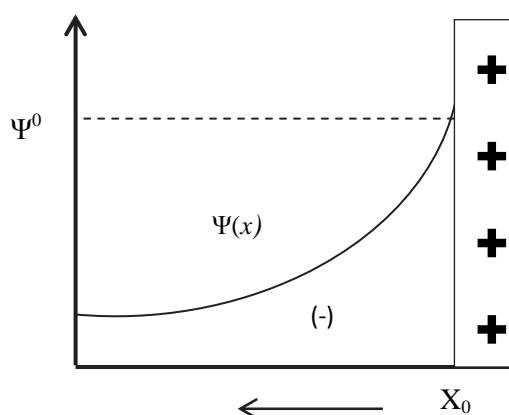


**Figure 3.4: Charge potential with distance from particle surface (Hunter, 1986)**

The Gouy-Chapman theory provides a better approximation of the double layer than the Helmholtz model, but still has its limitations. It characterises ions as point charges and assumes no physical limit in ion approach to the surface, which has been found to be unlikely (Stern, 1924 cited by Hiemstra et al., 1989). Stern modified the Gouy-Chapman diffuse double layer and stated that ions do have a finite size, so cannot approach a surface closer than the respective ion radius, a distance he termed  $\delta$ . With this modification the assumption of treating ions as point charges becomes justified. He also stated that some ions are specifically adsorbed by the surface in the plane  $\delta$ , a layer that has become known as the Stern Layer. This means that over the diffuse layer the potential will drop by  $\psi_\delta$ , a value that has become known as the zeta potential ( $\zeta$ ), which can be determined by electrophoresis. From these considerations the electrical diffuse double layer can be seen as a sheath of predominantly charged counter-ions around a charged colloid particle in suspension. The distance experiencing ion imbalance around the colloid particle depends on the charge potential of the colloid surface as well as the concentration of ions in the electrolyte. The ions that constitute the diffuse electrical double layer are referred to as the potential determining ions. In the case of the potential determining ions being either  $\text{OH}^-$  or  $\text{H}^+$  ions, it is possible to subject the particles to a value of pH at which the particle will have zero zeta potential. This point of pH is referred to as the isoelectric.

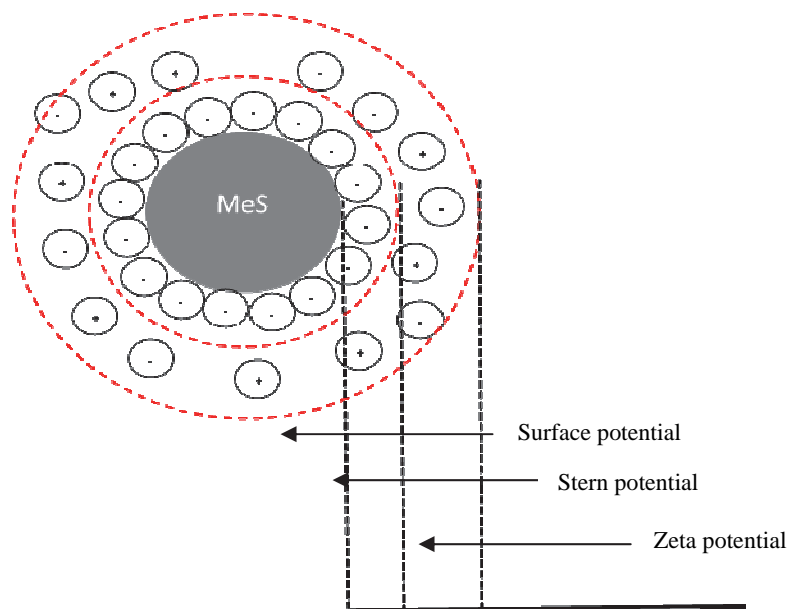


**Figure 3.5: Representation of the diffuse double layer (after Mehta et al., 2011)**

The potential profile around a charged particle is such that counter-ions are attracted and bound strongly to the particle surface and their concentration gradually falls away from the particle with increasing distance from the particle surface. The concentration of co-ions also gradually increases until it approaches the bulk concentration with increasing distance from the particle surface. A good representation of the electrical double layer is as presented by Mehta and co-workers (2011) shown in Figure 3.5.

### 3.9. Colloidal Stability

A colloidal dispersion is a heterogeneous system consisting of solid nanoparticles dispersed in a fluid medium. If the particles are small enough they undergo Brownian motion, resulting in continuous collisions with one another. The particles remain as single particles as long as the collisions do not result in permanent associations. The ability of the particles to remain as individual particles is termed colloidal stability and can be achieved by either of the following two ways.

- i. The particles can be given a charge potential, either negative or positive. If all the particles have the same charge they can repel each other to a lesser or greater extent when they approach each other. This is referred to as electrostatic stabilisation.
- ii. The particles can be coated with a polymer that always orientates the particles in such a way that when they collide, the particle centres are never close enough to result in permanent associations. This type of stabilisation is referred to as steric stabilisation.

Deryagin and Landau and Verwey and Overbeek (DLVO), independently developed a quantitative theory in which the electrical stability of colloidal dispersions was treated in terms of the energy changes that take place when particles with an electrical double layer approach one another (Shaw, 1970). The theory is based on net interaction energy ( $V_R$ ) due to an overlap of electric double layers (repulsion) and van der Waals forces (attraction) in terms of interparticle distance. If the electrical double layer (EDL) of two particles overlap in a typical Brownian motion encounter, Overbeek (1977) states that the rate of overlap is too fast for adsorption equilibrium of EDL ions to be maintained, resulting in a change of particle surface charge. For low surface potential ( $\psi_0 < 25$  mV),

the resultant potential energy of repulsion between two colliding particles is given by Everett (1988):

$$V_R^\psi = \frac{\pi\epsilon_0\epsilon_1\epsilon_2(\psi_1^2d_1\psi_2^2d_2)}{(a_1+a_2)} \frac{(2\psi_1\psi_2)}{(\psi_1^2d_1\psi_2^2d_2)} \ln\left(\frac{1+\exp[-kH]}{1-\exp[-kH]}\right) + \ln(1-\exp[-2kH]) \quad 8$$

where  $a_1, a_2$  relates to the radii of two spherical particles,  $H$  is the distance between the stern layers,  $c$  is concentration of electrolyte and  $k = \frac{zeNAcz^2}{\epsilon kT}$

For equal spheres  $a_1 = a_2$  Equation 8 reduces to Equation 9:

$$V_R^\psi = 2\pi\epsilon a\psi_d^2 \ln(1+\exp[-kH]) \quad 9$$

For higher potentials a more useful approximation is that given by Reerink and Overbeek (1954), which for unequal spherical particles is defined by Equation 10:

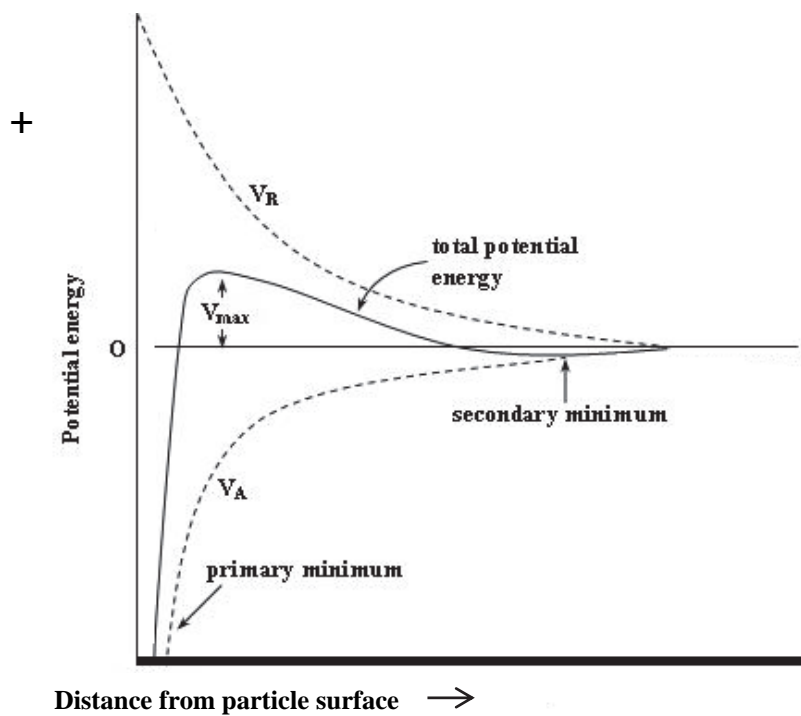
$$V_R = \frac{64\pi\epsilon a^1 a^2 k^1 T^2 \gamma^1 \gamma^2}{(a_1+a_2)\epsilon^2 z^2} \exp[-kH] \quad 10$$

This, for equal spheres reduces to Equation 11:

$$V_R = \frac{32\pi\epsilon a^1 a^2 k^1 T^2 \gamma^1 \gamma^2}{\epsilon^2 z^2} \exp[-kH] \quad 11$$

The summation of attractive (VA) and repulsive (VR) energies that gives the net interaction energy between two colliding particles is shown in

Figure 3.6, where net interaction energy is plotted against distance of two colliding particles. A positive potential indicates a dominant repulsive force, whereas a negative potential indicates a dominant attractive force. The primary minimum corresponds to the minimum in the energy curve at the left hand side of the energy barrier while the secondary minimum is usually not sufficiently deep to withstand re-dispersion of particles by Brownian motion. Electrophoretic mobility, measured by zeta potential, can be used as measure of the electrostatic forces experienced by colloidal particles in solution.



$V_R$  is Repulsive force  
 $V_A$  is Attractive force  
 $V_{max}$  is the maximum repulsion experienced by particles

**Figure 3.6: The net interaction energy between two colliding particles (Hunter, 1986)**

### 3.10. Electrophoresis

Electrophoresis refers to the motion of suspended particles in response to an applied electric field. An isolated ion in an electric field would experience a force ( $F_{el}$ ) directed toward the oppositely charged electrode as defined by Equation 12:

$$F_{el} = qE \tag{12}$$

Where  $q$  is the charge of the ion and  $E$  is the electric field in  $V\ m^{-1}$ .

The velocity of the particle is proportional to the applied field strength and in the case of a spherical particle takes the form of Equation 13:

$$v = \mu_E E \tag{13}$$

where  $\mu_E$  is electrophoretic mobility of the particle (Hunter, 1986). Zeta potential as measured by the Zetasizer is a function of the electrophoretic mobility.

### 3.11. Particle size distribution analysis technique

A technique described by Randolph and Larson (1988) based on the population density function,  $n(L)$ , was used to derive and describe PSD related information. The number of particles in a given size range is given as a function represented by Equation 14:

$$n(L) = \frac{dN}{dL} \tag{14}$$

From a volume based histogram (vol% versus  $L_i$ ), the density function is calculated according to Equation 15:

$$n(L) = \sum_i \frac{\text{vol}\% \times \text{conc}(\text{vol}\%)}{100} \cdot \frac{1}{k_v L^3} \quad 15$$

Where  $i$  indicates the size sub-range and the particle concentration is represented by  $\text{conc}(\text{vol}\%)$ . A volume factor ( $k_v$ ) equal to  $\pi/6$  is used to take into account the sphericity of the particles.

$$m_j = \int_0^{\infty} L^j n(L) dL \quad j = 0, 1, 2, 3, \dots \quad 16$$

Equation 16 defines the  $j$ th moment of the number density function with respect to its internal coordinate,  $L$ . From integration of Equation 16, the zeroth moment ( $m_0$ ), first moment ( $m_1$ ), second moment ( $m_2$ ) and third moment ( $m_3$ ) are obtained. The zeroth moment is equal to the total number of particles, and the first, second and third moments are proportional, respectively, to total length, total surface area and volume of the particular matter. The number based mean size of the particles was determined from the zeroth and first moment as defined by Equation 17:

$$\bar{L}_{1,0} = \frac{m_1}{m_0} \quad 17$$

## 4. Literature Review

Metal sulphide precipitation is an important process in hydrometallurgical treatment of ores and effluents (Lewis, 2010). Due to its relative simplicity and low costs, hydroxide precipitation is widely used in industry (Huisman et al., 2006). Advantages of metal sulphide precipitation include potential selective precipitation of metals, lower solubility of metal sulphide precipitates, better settling properties, in the case of some sulphides, and fast reaction rates. Reuse of metals can only become economically and technically feasible when metals are removed selectively and relatively pure metal sludges are produced, all of which are attributes of metal sulphide precipitation (Veeken et al., 2003). Sulphide precipitation can be effected using either solid (FeS, CaS), aqueous (Na<sub>2</sub>S, NaHS, NH<sub>4</sub>S), gaseous (H<sub>2</sub>S) or the degeneration reaction of Na<sub>2</sub>S<sub>2</sub>O<sub>3</sub> as potential sulphide sources. Metal sulphides are normally characterised by low solubility and a high affinity between the reactants, which leads to high supersaturation driven reactions. Veeken and co-workers (2003) stated that if the amount of sulphide was not in stoichiometric quantities with the amount of metal, either excess of metals or excess sulphide would remain in solution. In cases where stoichiometric quantities of metal and sulphide are reacted, a challenge of controlling supersaturation may still exist. When H<sub>2</sub>S gas was bubbled into a contactor filled with wastewater, extreme supersaturation of sulphide was dominant at the points of gas injection, this led to metal sulphide particles smaller than 10 µm characterised by poor settling (Mersmann, 1999), while Mokone and co-workers (2010) reported relatively large metal sulphide particles with good settling characteristics at low supersaturation conditions. This suggests that high supersaturation favours high nucleation rates as compared to crystal growth.

Mokone and co-workers (2010) investigated the effect of solution chemistry on particle characteristics during metal sulphide precipitation and presented the results of change in zeta potential as a function of metal to sulphide ratio as shown in Figure 4.1. The results depicted the particle charge of particles which remained in suspension after settling. The zeta potential of both the copper and zinc sulphide particles became less negative with an increase in the metal to sulphide molar ratio. The magnitude of the zeta potential for copper sulphide particles was larger than that of the zinc sulphide particles produced under similar conditions, while for copper sulphide particles, the zeta potential of particles produced in excess sulphide were substantially more negative than that of particles produced under sulphide deficient conditions.

Mokone et al. (2010) suggested this to be consistent with high supersaturation conditions, resulting in rapid nucleation of a large number of charged particles, followed by adsorption of excess sulphide onto the particle surface, imparting the relatively large negative charge. The formation of a large number of particles is supported by Sohnel and Garside (1992) who stated that supersaturation is the thermodynamic driving force behind every precipitation process and the level of supersaturation in a precipitating system governs the particle rate process, such as nucleation, growth and aggregation and by Kolthoff and Moltzau (1935) who observed that metal sulphides strongly absorbed sulphide ions.

The extent of aggregation of a suspension can be investigated by several ways which include: settling rate (Vergouw et al., 1997), viscosity (Muster and Prestidge, 1995), optical microscopy (Adler, 1987), particle size distribution (Lange et al., 1997), atomic microscopy (Muster et al., 1996) and turbidity (Maroto and de las Nieves, 1998). Mokone and co-workers (2010) reported a large increase in the surface area of copper sulphide particles when precipitation was carried out in excess sulphide conditions as shown in Figure 4.2. This change was attributed to the inhibition of

aggregation and, according to the DLVO theory, the colloidal dispersion was most likely experiencing relatively large electrostatic forces. Mokone and co-workers (2010) stated that aggregation of colloid particles was inhibited when the zeta potential of colloid particles surpasses a certain value, which they suggested to be -40 mV.

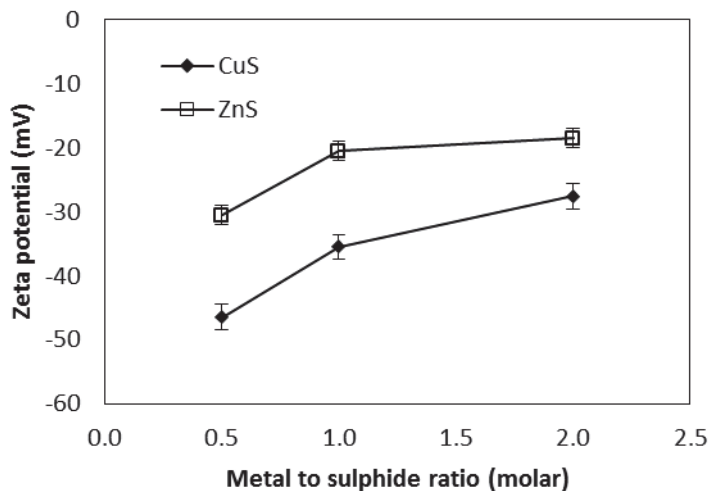


**Figure 4.1: Change in zeta potential of metal sulphide as a function of metal to sulphide ratio at pH6 (Mokone et al., 2010)**

Mokone et al. (2010) reported a zeta potential of -46 mV for a CuS system and -30 mV for a ZnS system under identical reaction conditions, a metal to sulphide ratio of 0.5 and pH of 6. They attributed this to the selective adsorption of  $\text{HS}^-$  and  $\text{S}^{2-}$  ions on the CuS particles, resulting in a more negative potential. Zeta potential is a function of electrolyte concentration, particle surface charge and pH (Hunter, 1986). If operating conditions are kept constant, electrolyte concentration and pH become fixed. For both systems, simulation software showed  $\text{Zn}^{2+}$  and  $\text{Cu}^{2+}$  to be the most abundant metal sulphide products. This means that the ZnS and CuS systems are comparable and an investigation into why the respective zeta potentials differ is valid.

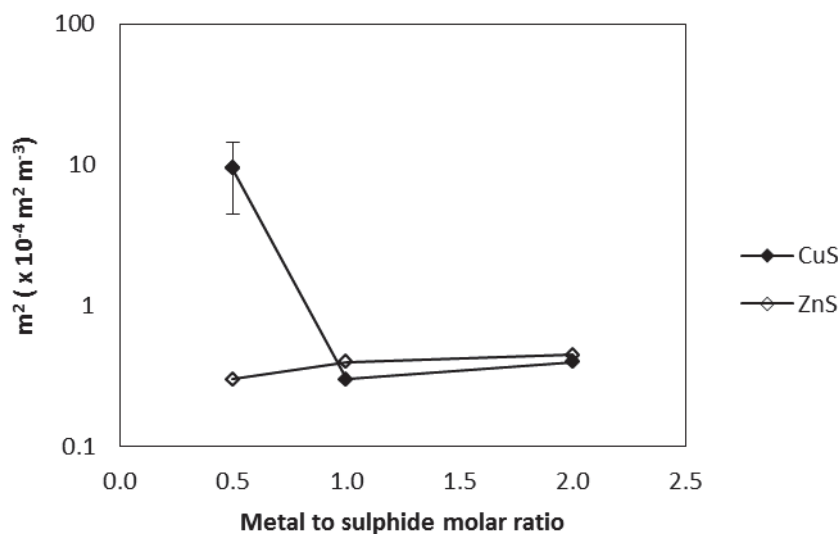


**Figure 4.2: Change in the  $m^2$  (related to surface area) for metal sulphide precipitates with different metal to sulphide ratios (Mokone et al., 2010)**

In order to obtain precipitate particles with good settling characteristics, effective control of the precipitation process is necessary. Effects of high supersaturation can be controlled by techniques that effectively reduce and spread supersaturation throughout the reactor. Taty-Costodes and Lewis (2006) used this approach and effectively spread supersaturation by employing the use of multiple reagent feed points, resulting in a reduced amount of small particles or fines of nickel hydroxyl-carbonate. This technique was also successfully employed by Sampiao and co-workers (2010), in the precipitation of nickel and zinc. However, Mokone and co-workers (2012) found that spreading the supersaturation by using multiple feed points had no significant effect on the amount of small metal sulphide particles leaving the reactor as fines. During industrial precipitation, effective control of supersaturation may be difficult and in such cases post precipitation techniques should be adopted or developed to aid with solid-liquid separation. They presented the case that, this would also be necessary in the event that manipulating supersaturation in-situ has a minimal effect on the settling particles of formed colloid particles.

## **5. Experimental Studies**

### **5.1. Analytical Methods**

#### **5.1.1. Zeta potential measurements**

All zeta potential measurements were measured using electrophoresis via the Malvern Zeta Sizer (Nano ZS model).

#### **5.1.2. pH measurements**

The pH was measured using a Microprocessor pH meter (pH 212, Hanna instruments). The pH electrodes were calibrated at pH 4 and 10 using Merck standard buffer solutions before every experiment.

#### **5.1.3. Sulphide analysis**

Total dissolved sulphide concentration was measured spectrophotometrically at 670 nm, following the colour development of methylene blue resulting from the reaction between the sulphide and the colorimetric reagent (*N,N*-dimethyl-*p*-phenylenediamine sulphate) in acid medium. Ferric chloride was used as a catalyst for this reaction. An appropriate volume of the sample was added to 200  $\mu\text{L}$  of 1% zinc acetate immediately after the sample was collected from the reactor. This was diluted up to 5 mL using de-oxygenated water. A volume of 500  $\mu\text{L}$  *N,N*-dimethyl-*p*-phenylenediamine hydrochloride solution and 500  $\mu\text{L}$  of ferric chloride were added to the diluted sample. The sample was then thoroughly mixed and allowed to react for 15 minutes before concentration was measured using a Merck Spectroquant® NOVA 60.

## 6. Studies to investigate effect of reaction conditions on particle characteristics

### 6.1. Objective

This investigation has been previously done by Mokone and co-workers (2010), but because it forms part of the basis of the current work it was repeated to ensure reproducibility and to form a baseline for further studies.

### 6.2. Materials and methods

#### 6.2.1. Reagents

Solutions were made up to the required concentrations using Millipore de-ionised water that was initially boiled to a temperature of 80°C and left to cool in a closed vessel. Reagents used were all analytical grade chemicals branded Merck and Sigma-Aldrich, namely  $\text{Na}_2\text{S}\cdot 9\text{H}_2\text{O}$ ,  $\text{CuSO}_4\cdot 5\text{H}_2\text{O}$ ,  $\text{NiSO}_4\cdot 6\text{H}_2\text{O}$ ,  $\text{ZnSO}_4\cdot 7\text{H}_2\text{O}$ ,  $\text{CaCl}_2$ ,  $\text{Al}_2(\text{SO}_4)_3\cdot 18\text{H}_2\text{O}$ ,  $\text{KCl}$ ,  $\text{HCl}$  and  $\text{NaOH}$ . All prepared solutions were sparged with nitrogen before use.

#### 6.2.2. Experimental setup

A 1 litre glass vessel with a working volume of 0.9 L was used as a continuously stirred tank reactor vessel. The vessel was equipped with a perspex lid with six ports to accommodate an agitator, pH probe, reagent dosing nozzles, nitrogen sparger and pH controller dosing nozzle. Mixing was achieved by a Rushton turbine connected to an overhead stirrer with variable RPM. The impeller used had four blades with a 5.6 cm diameter and the reactor was equipped with four baffles. The six ports on the lid were to cater for a pH electrode, impeller shaft, nitrogen gas inlet and reagent inlet. A Metrohm 800 Dosino pH stat device, in combination with a sulphide resistant pH electrode was used for measuring and controlling pH. The dosing device controlled pH by automatic addition of either 0.5 M HCL or 1.0 M NaOH. Metal and sulphide reagents were pumped in to the reactor using calibrated Watson Marlow 520S (Falmouth, UK) pumps.

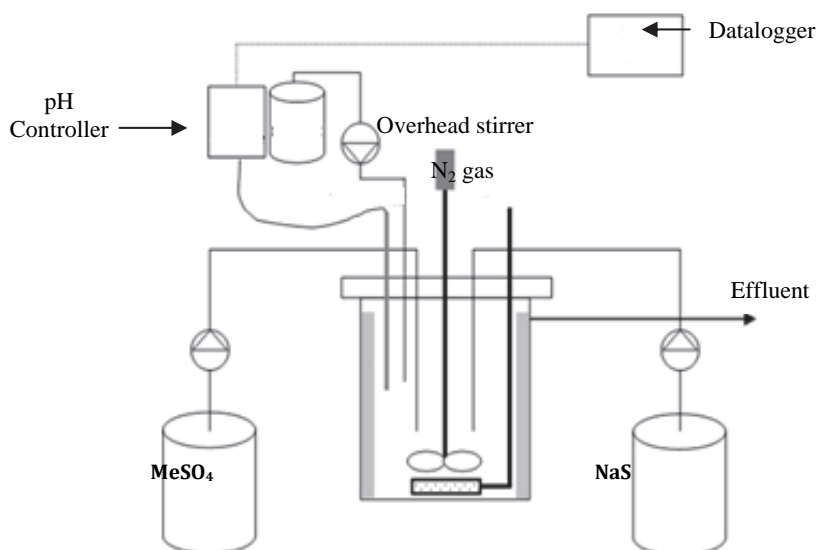


Figure 6.1: Experimental setup for the precipitation of metal sulphide particles

### 6.2.3. Experimental Procedure

Reagent stock solutions were prepared using Millipore de-ionised and deoxygenated water. Metal ion concentration was kept constant at  $500 \text{ mg.L}^{-1}$ . All experiments were conducted at room temperature. The experiments were carried out in a 1 litre glass continuous stirred tank reactor with a working volume of 900 mL. The reactor was filled with 900 mL of Millipore de-ionised water and bubbled with nitrogen gas for an hour to remove oxygen. Before addition of any reagents the nitrogen gas flow rate was reduced, but still significant enough to maintain a slight positive pressure in the reactor. The overhead stirrer was set at 620 rpm then the reagents were pumped in to the reactor at the same flow rate of  $50 \text{ mL.min}^{-1}$  achieving a residence time in the reactor of about 9 minutes. Reactor pH was kept constant at a pH of 6 and experiments were repeated three times to ensure reproducibility. Metal to sulphide ratio (molar) was varied for both zinc and copper sulphide systems at ratios of 0.5, 1.0 and 2.0.

### 6.3. Results and Discussion

This work (Figure 6.2) showed the same general trend as demonstrated by Mokone et al. (2010). However, the respective zeta potential values of the metal sulphide particles in the repeated experiments were more negative than those reported by Mokone et al. (2010) under similar reactor conditions. The zeta potential of the formed particles became less negative, with an increase in the metal to sulphide ratio for both copper and zinc sulphide systems. The magnitude of the zeta potential of copper sulphide was however higher than that of the zinc sulphide particles under similar conditions. Differences in the zeta potential between original and repeated measurements could have arisen from effects of partial oxidation during sample manipulation and analysis, or slight changes in solution chemistry. Partial oxidation alters the surface chemistry of the metal sulphide particles resulting in an increase in zeta potential and may not necessarily result in full oxidation of the metal sulphide which would result in the formation of a sulphate. The zeta potential of copper sulphide and zinc sulphide particles became more negative with an increase in excess aqueous sulphide because of an increase in the adsorption of sulphide ions on to the colloid particle surfaces, as proposed in the review of literature.

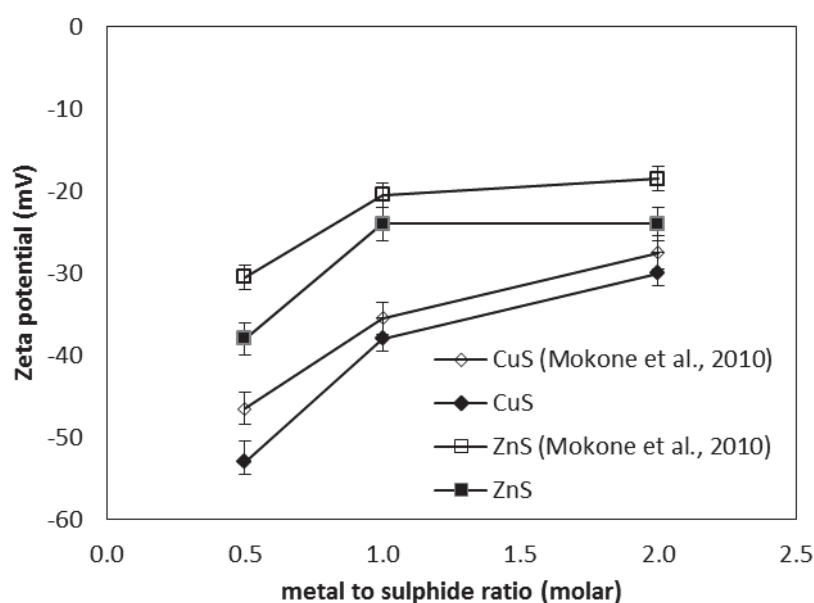


**Figure 6.2: Change in zeta potential of metal sulphide particles as a function of metal:sulphide molar ratio at pH 6 compared with Mokone et al. (2010)**

Nickel sulphide was added to the investigation (Figure 6.3) in order to try and develop a trend and understand how charge development in metal sulphide systems changes with a change in solubility. The zeta potential of nickel at all three metal:sulphide ratios was very unstable and hence a trend was difficult to identify. The reason behind nickel sulphide exhibiting such unstable characteristics could be attributed to factors observed and stated by Bhattacharyya and Chen (1986), who observed that nickel sulphide was prone to surface oxidation and successful precipitation was possible at  $\text{pH} > 8$  under a closed reactor. Bhattacharyya and Chen (1986) also stated that precipitation of metals such as nickel and cobalt was complex because of post dissolution of nickel sulphide and cobalt sulphide. The above reaction was carried out at a pH of 6, which may not have been ideal for successful precipitation of nickel sulphide. This is further supported by subsequent experiments in the current work (Figure 7.1, Page 29) which show that nickel sulphide particles had a zeta potential of -40 mV, with minimal deviation, at a pH value close to 9.

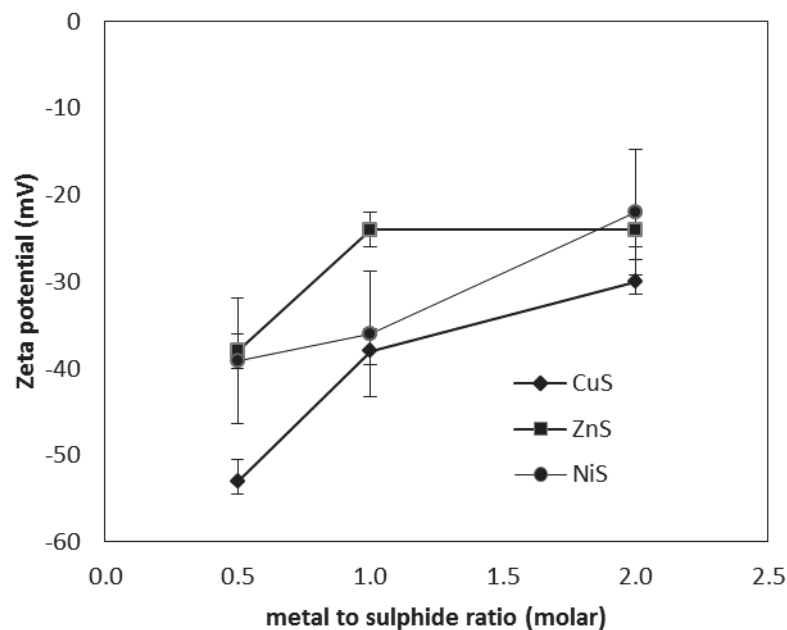


**Figure 6.3: Change in zeta potential of metal sulphide particles as a function of metal:sulphide ratio**

#### 6.4. Conclusions

The current results agreed with Mokone and co-workers (2010). An increase in the amount of sulphide ions at a constant metal ion concentration in solution during metal sulphide precipitation was shown to have a significant effect on formed particles resulting in small highly charged particles with poor settling characteristics. Colloid surface charge was strongly influenced by sulphide ions present in solution and this affected copper sulphide particles to a larger extent than the zinc sulphide particles. This could have been due to the selective adsorption of sulphide ions on copper sulphide particles when sulphide was in excess, but further investigations are needed to verify this. Aggregation was inhibited when primary metal sulphide particles possessed a zeta potential more negative than a certain threshold value. The results were consistent with the findings of Dekkers and Schoonen (1994) after investigating the effect of changing the metal to sulphide ratio on zeta potential of metal sulphides. They noted that as the concentration of sulphide ions became more than that of the metal ions, the zeta potential of the respective particulates became more negative, the opposite was also found to be true.

## **7. Studies to investigate whether or not there is a specific zeta potential value at which aggregation is suppressed**

### **7.1. Objective**

Aggregation inhibition of colloidal particles was investigated by observing the PSD of colloidal particles produced at different pH values, for three different metals: copper, nickel and zinc.

### **7.2. Materials and methods**

The reagents and reactor set-up are described in detail in Sections 6.2.1 and 6.2.2

#### **7.2.1. Experimental procedure**

Reagent stock solutions were prepared using Millipore de-ionised and deoxygenated water. Metal ion concentration was kept constant at 500 mg.L<sup>-1</sup>. All experiments were conducted at room temperature (25°C) and the equipment was setup as described in section 6.3. The pH was varied for Cu (pH 5.0-6.0, 0.2 increments), Zn (pH 6-8, 0.2 increments) and Ni (pH 6.0-8.0, 0.2 increments). Supersaturation was kept constant for all experiments, at a metal to sulphide molar ratio of 0.5. In the current investigation, Particle Size Distribution (PSD) was used as a measure of aggregation and colloidal stability.

An online sulphide probe giving real time sulphide concentration inserted in the reaction vessel was used to ascertain steady state. After steady state the precipitate solution was sampled at 10 min intervals over a period of 60 min. The sample was collected from the effluent stream with a portion of this being used for PSD analysis and another portion being used to measure zeta potential. The PSD results were only used as a measure of aggregation.

### **7.3. Results and Discussion**

All the results reported were obtained after the process had achieved steady state, determined by a constant sulphide concentration, and for all three metals this was after 25 minutes. Aggregation was deemed to be inhibited when precipitant material remained stable in suspension. The zeta potential values at which NiS, ZnS and CuS formed stable suspensions are shown in Figure 7.1. Statistical variation of the results is shown by error bars which represent standard error of reported zeta potential values after three independent runs. The least negative value of zeta potential at which aggregation was inhibited was -36.2 mV which was observed for NiS while the most negative value, -40.1 mV, was observed for CuS. Zinc sulphide particles formed a stable suspension at intermediate value of -38.1 mV.

The results indicate that a certain threshold value, an average of -38 mV ± 2 mV, was necessary for aggregation to be inhibited. This is consistent with the findings of Muster and Prestidge (1995), who observed maximum aggregation at the isoelectric point of a sphalerite system. The results also confirm that nickel, copper and zinc sulphide systems obey the DLVO theory. Consequently, aggregation may be promoted or inhibited by altering the zeta potential of the precipitant particles. However, DLVO interactions may be affected by various other factors. Hydration of surface species can induce a repulsive effect while hydrophobic surface species can induce aggregation (Mirnezami et al., 2003). This supported earlier findings by Vergouw and co-workers (1998) who observed maximum aggregation (via settling rate) for ZnS at pH 10 and a zeta potential of -40 mV. They

suggested that a hydrophobic force was induced that was sufficient to overcome the electrostatic repulsion. This highlights the fact that in certain cases it may be necessary to look beyond DLVO forces in explaining the settling characteristics of colloidal suspensions. In the case of the reported metal sulphides, NiS, CuS and ZnS, it appears that the respective precipitant material obeys the DLVO theory. However, the reported value at which aggregation is inhibited is only valid for the specific reaction conditions stated in the experimental procedure. This is because even for DLVO systems, aggregation is affected by other factors such as solution ionic strength, solids density and solution redox conditions. As such, a variation in any one of these solution properties can lead to a shift in the zeta potential value at which aggregation is inhibited.

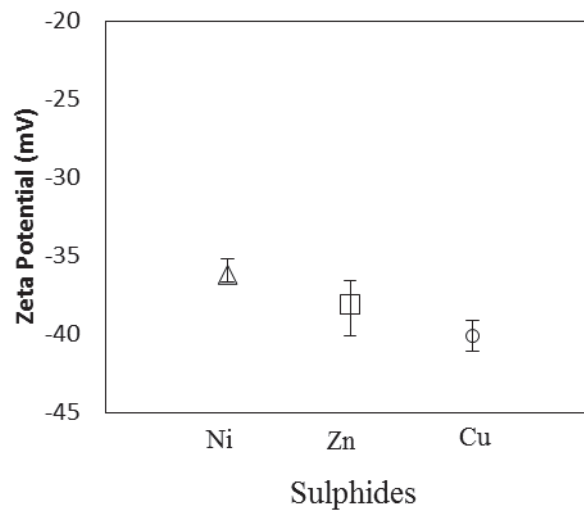


**Figure 7.1: Zeta potential values at which aggregation is inhibited**

#### 7.4. Conclusions

Surface properties of colloidal particles including surface charge development is a prerequisite for the transformation of reactants via surface mediated reactions. Aggregation in colloidal dispersions generally obeys the DVLO theory and stability depends on the resultant interaction between repulsive and attractive forces of colliding particles. The zeta potential of colloidal particles was altered by effectively changing the operational reactor pH. As pH was increased, the zeta potential of the particles became more negative. This resulted in an increase of the inter-particle repulsive forces leading to a reduction in particle size. After a zeta potential value of about  $-38 \text{ mV} \pm 2 \text{ mV}$  was attained aggregation was inhibited. The zeta potential value depends on operational pH and supersaturation and is specific only for the specified conditions. The greater significance of this is that every colloidal system has a zeta potential value at which the primary particles experience a repulsive force much greater than the van der Waals forces of attraction. This results in sulphide particles with a small mean size and generally poor settling characteristics.

## 8. Effect of post-precipitation conditions on surface properties of colloidal metal sulphide particles

### 8.1. Materials and Methods

The reagents are described in detail in Section 6.2.1.

#### 8.1.1. Experimental set up

All metal precipitation reactions were conducted in a 2.0 litre glass vessel operated as a semi batch reactor and equipped with four equally spaced baffles. The reactor was operated as a closed reactor with 6 ports on the lid for reagent inlet, pH electrode, impeller shaft and nitrogen gas inlet. Agitation was achieved using an overhead stirrer running at 620 rpm fitted with a Rushton turbine.

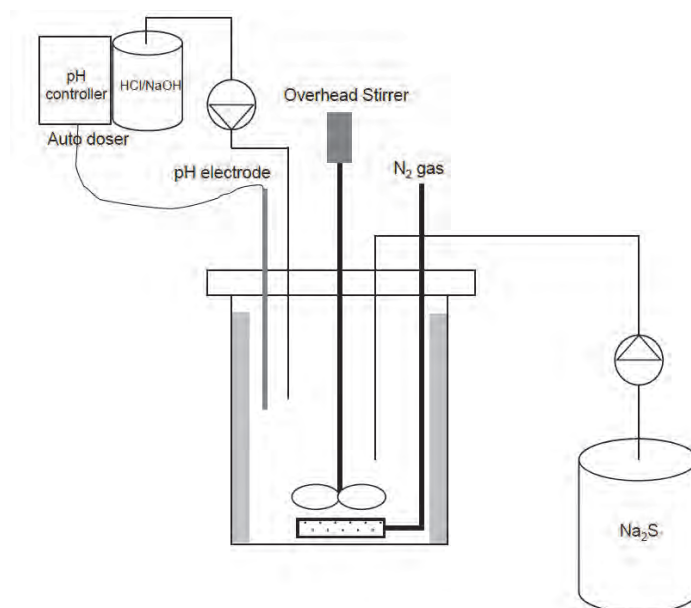


**Figure 8.1: Semi batch experimental set-up for the precipitation of metal sulphide particles**

#### 8.1.2. Experimental procedure

The experimental design was divided into two phases. The first phase involved sulphide precipitation of copper and zinc ions using aqueous sodium sulphide in a semi batch reactor. In the second phase three effects on particle characteristics were studied:

- i. The effect of suspension pH
- ii. The effect of sulphide addition
- iii. Effect of divalent and trivalent cations

The change in surface properties was characterised by using the change in zeta potential and the mean size of the particles was analysed using particle size distribution. KCl was used as the background electrolyte for all the experiments.

The experiments investigating the effect of suspension pH were conducted at 1, 10 and 100 mM electrolyte concentrations while pH was varied between pH 2.5 and 11 using either NaOH or HCl. Sulphide addition was within the range 0-7 mM at 1 mM intervals while background electrolyte concentration was kept at either 10 or 100 mM. The cation addition experiments were carried out by

suspending the precipitates in 10 mM background electrolyte solution and adding the cations at varying concentrations ranging between 0-5 mM at 1 mM intervals.

### 8.1.3. Metal Precipitation

The reactor was filled with 1.5 L of the standard metal sulphate solution at a fixed concentration of 2000 mg.L<sup>-1</sup> of either copper or zinc. The reactor contents were then bubbled with nitrogen for 20 minutes to achieve sufficient de-oxygenation after which the nitrogen flow rate was reduced to minimise bubble formation and particle flotation. Sodium sulphide at 3500 mg.L<sup>-1</sup> was titrated in the reactor using a pre-calibrated Watson Marlow 520S pump at a flow rate of 11.5 mL.min<sup>-1</sup>. Reactor pH was controlled at pH 4.5 for copper sulphide and pH 6.0 for zinc sulphide precipitation using a pH stat device, Metrohm 800 Dosino connected to a computer with control software tiamo<sup>TM</sup> version 1.2, Metrohm AG, Switzerland.

The synthetic sulphide solution was titrated into the reactor until stoichiometric amounts of metal:sulphide were achieved. A 20 mL sample was withdrawn from the reactor after 10 min of sulphide addition and filtered through a 0.2 µm pore size filter. The filtrate was used to determine metal ion concentration using atomic adsorption spectroscopy (VarianSpectrAA 110). The rest of the reaction mixture was freeze dried for 48 hours then washed several times with de-oxygenated water to remove excess ions. The final suspension was freeze dried for another 48 hours to minimize oxidation, and the precipitates were stored in an oxygen-free environment.

### 8.1.4. Surface studies

The reactor was filled with 650 mL of background electrolyte solution and nitrogen was sparged through it for 20 min to achieve de-oxygenation, after which the nitrogen flow was reduced to minimise bubble formation and possible particle flotation. The precipitate was transferred to the reactor as a 100 mL suspension consisting of 0.25 g of the metal sulphide precipitate. After the suspension addition the reactor was allowed to equilibrate for 20 minutes before any further treatment or analysis.

Statistical analysis of all the results was evaluated using the standard error. All experiments were done in triplicate and the reported values were the average of all recorded independent runs while the respective standard error was displayed as error bars in all applicable graphs.

## 8.2. Results and discussion

### 8.2.1. Effect of pH on surface properties

Figure 8.2 shows the change in zeta potential as a function of pH for both copper and zinc precipitates suspended in different concentrations of background electrolyte solutions. Both metal precipitates exhibit negative zeta potential, indicating minimal oxidation of the metal sulphides (Healy and Moignard, 1976; Fairthorne et al., 1997). In the case of copper, Figure 8.2, the magnitude of the zeta potential increased when pH was increased for the 1 and 10 mM suspensions. The zeta potential of the particles suspended in the 100 mM background electrolyte became less negative at pH 6, and according to Clarke and co-workers (1995) this is consistent with the surface becoming increasingly covered with metal oxide/hydroxide species due to surface oxidation. This is possible because of residual oxygen in the solution after nitrogen sparging. To verify this phenomenon, thermodynamic modelling (Visual Minteq ver. 3.0) was conducted to determine if

formation of metal oxide/hydroxide was possible over the full spectrum of operating conditions. The results showed dissociation of copper ions and formation of different aqueous copper hydroxide species and copper chloride (i.e.  $\text{CuCl}^+$ ,  $\text{CuCl}_3^-$ ,  $\text{CuCl}_4^{2-}$ ) complexes. The concentration of these complexes was shown to be dependent on pH and concentration of the background electrolyte.

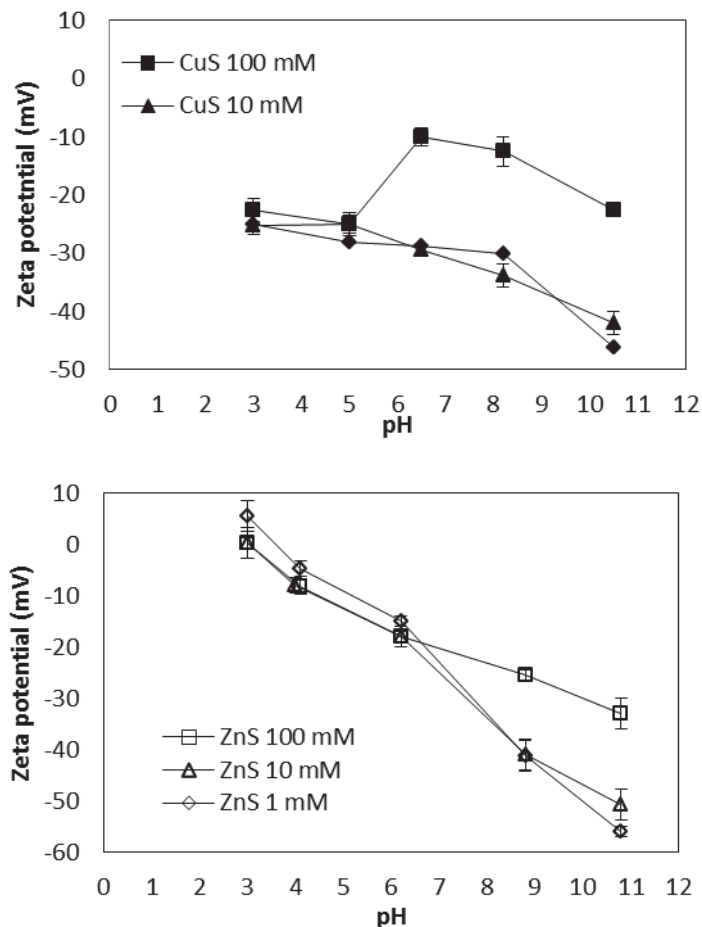


**Figure 8.2: Change in zeta potential as a function of pH for CuS and ZnS**

The concentration of  $\text{Cu}_2\text{OH}^{3+}$  complex was found to be very high, reaching a maximum at pH 6 for 100 mM background electrolyte concentration experiments. The adsorption of this positively charged complex onto the surface of the particles was suggested as the possible reason for the observed change in zeta potential becoming less negative.

According to Senanayake (2009), oxidation of sulphide minerals involves surface reaction mechanisms via the formation of mixed-ligand complexes in the form of adsorbed or dissolved species (e.g.  $\text{Cu}(\text{OH})\text{Cl}$ ). Surface adsorbed chloride ions are involved in the surface reaction and the rate of the surface chemical reaction is dependent on the chloride ion concentration. As such, copper oxide/hydroxide due to chloride-induced surface oxidation of the particles was seen as another possible reason behind the increase in zeta potential at pH 6 and 100 mM background electrolyte concentration. At lower background electrolyte concentrations (1 and 10 mM, KCl), the trends observed were similar to those of elemental sulphur (Healy and Moignard, 1976), which exhibited limited surface oxidation.

For the zinc precipitate, zeta potential became more negative with an increase in pH. The change in magnitude of zeta potential for both 1 and 10 mM electrolyte suspensions with an increase in pH was almost the same. At pH 6, however, the magnitude of the zeta potential increase was lowered for experiments run with the 100 mM electrolyte suspension.

At pH 3.5, the zeta potential of zinc was close to zero, indicating the isoelectric point of the particles. Williams and Labib (1985) and Nicolau and Menard (1992) also report a similar pH value for the isoelectric point for synthetic zinc sulphide particles. The consistent decrease in the magnitude of the zeta potential suggests minimal oxidation of particle surfaces. The observed decrease in the magnitude of zeta potential increase when pH was above 6 for the 100 mM electrolyte suspension was attributed to the compression of the electrical double layer as the ionic strength of the suspension increased.

The quantitative theory of colloid stability states that particle aggregation, governed by the DVLO theory, is enhanced when particles have close to zero zeta potential. On the other hand, particle size increases while surface area of particles decreases due to formation of particle clusters. Figure 8.3 and Figure 8.4 illustrate that the change in the number based mean size ( $\bar{L}_{1.0}$ ) and second moment ( $m_2$ -equivalent to surface area) as a function of pH for copper and zinc precipitates suspended in different concentrations of background electrolyte solutions.

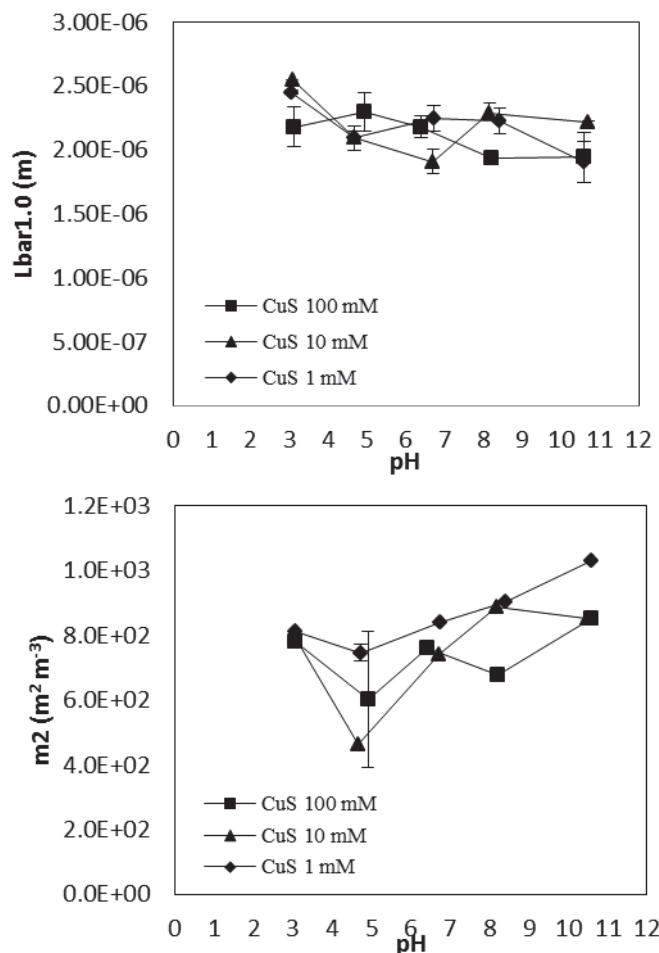


**Figure 8.3: Change in  $m_2$  and number based mean of CuS particles with pH**

The change in pH of the suspension and the concentration of background electrolyte had an effect although not significant on both  $\bar{L}_{1.0}$  and  $m_2$ . A slight decrease in  $\bar{L}_{1.0}$  was observed when pH was increased from 2.5 to 4 in the case of zinc and when pH of the suspension was above 4 the change in  $\bar{L}_{1.0}$  was negligible for all background electrolyte concentrations. In the case of copper, a small decrease in  $\bar{L}_{1.0}$  was initially obtained for the 1 and 10 mM suspensions when pH increased from 3.0 to 4.5. The change however, became erratic when pH was above 4. This was attributed to the possible formation of copper hydroxide due to the precipitation of dissociated  $\text{Cu}^{2+}$ , liberated from hydroxysulphate component of the precipitate. The  $\bar{L}_{1.0}$  obtained for the zinc sulphide precipitate was found to be generally smaller than that obtained for the copper precipitate. This was consistent with results shown in Figure 8.2 which demonstrated that the magnitude of the negative zeta potential increase was higher for the zinc precipitate.

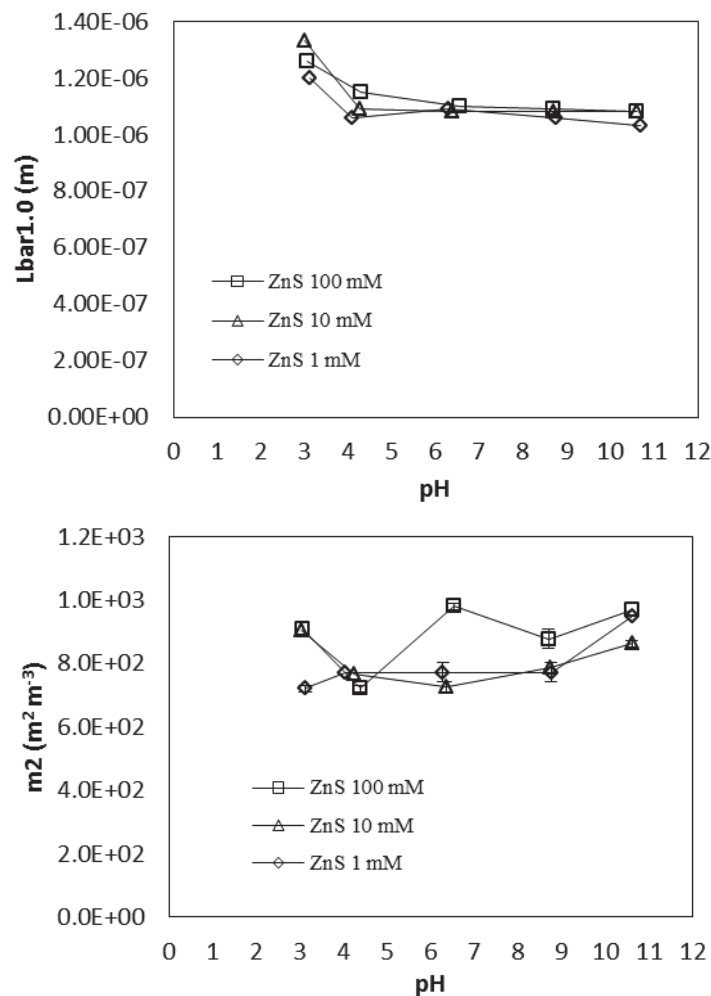


**Figure 8.4: Change in  $m_2$  and number based mean of ZnS particles with pH**

In the case of copper, when pH was increased from 3 to not more than 0.2 units above 4,  $m_2$  also decreased with the largest change being observed for the 10 mM suspension (Figure 8.3). The change in  $m_2$  at pH 4.5 for the 100 mM suspension was difficult to interpret due to a large error in the results, possibly due to the presence of hydroxysulphate in the precipitate. Above a pH of 4.5, the general trend was an increase in  $m_2$  with an increase in pH of the suspension. The magnitude of increase was slightly affected by background electrolyte concentration although this was not clearly defined as shown in the results. For the zinc precipitate (Figure 8.4) an initial decrease is observed

when pH is initially changed from 2.5 to 4.0, in the case of 1 and 10 mM suspensions. Above a pH of 4.0, the general trend was a slight increase in  $m_2$  although no strong trend was observed. This increase was slightly higher than that observed for the copper system, it was postulated that this was due to the formation of additional surface area, as a result of copper hydroxide formation.

### 8.2.2. Effect of sulphide addition on surface properties

As shown in Figure 8.5, the zeta potential in both metal systems became more negative with an increase in sulphide concentration. For the copper suspension however, the increase in zeta potential (less negative) was observed only up to a concentration of 3 mM, after which zeta potential remained relatively unchanged with further sulphide addition. The difference in zeta potential between the two electrolyte solutions for copper was less pronounced for all sulphide concentrations. In the case of zinc, addition of a small amount of sulphide resulted in a significant initial change in zeta potential (more negative), while further sulphide addition resulted in a suppressed change in zeta potential. This was generally the trend for both electrolyte concentrations although zeta potential for the 100 mM background electrolyte was less negative than for the 10 mM electrolyte system.

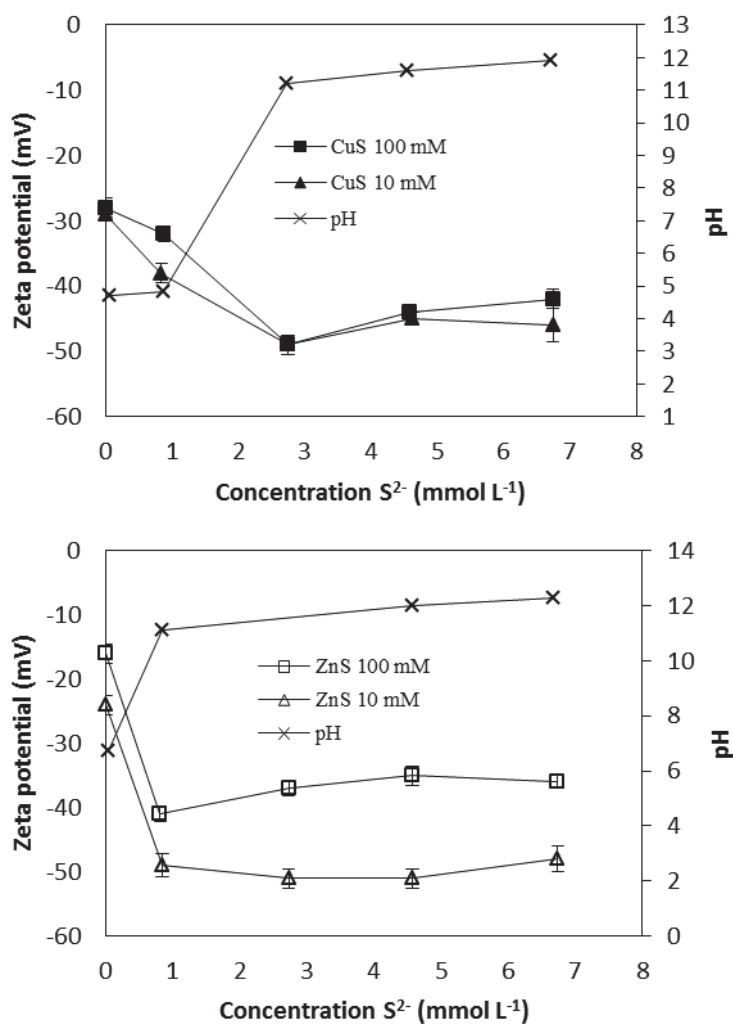


Figure 8.5: Change in zeta potential with sulphide concentration

When sulphide was added to the suspension, zeta potential became more negative suggesting adsorption of the negatively charged sulphide species (i.e.  $\text{HS}^-$  and/or  $\text{S}^{2-}$ ). The fact that zeta potential remained relatively unchanged after further addition of sulphide could be attributed to the saturation of free sulphide adsorbing sites on the surface of particles. This corroborates Newel and co-workers (2007), who studied sulphidisation of oxidized metal sulphides and found that the process was associated with strong chemisorption of the negatively charged bi-sulphide ions through anionic exchange. The small change in zeta potential obtained when a small amount of sulphide was added to the copper suspensions was attributed to the consumption of the added sulphide by the  $\text{Cu}^{2+}$  ions dissociated from the copper hydroxysulphate component of the precipitate.

### 8.2.3. Effect of cation addition on surface properties

The results in Figure 8.6 show the change in zeta potential and the pH of the suspension when different concentrations of  $\text{Al}^{3+}$  and  $\text{Ca}^{2+}$  are added to the 10 mM suspensions of copper and zinc precipitates. With addition of a small amount of  $\text{Al}^{3+}$  ions, the zeta potential of the particles became significantly less negative for both copper and zinc particles while pH also decreased in both cases. Zeta potential became slightly less negative with an increase in the amount of  $\text{Ca}^{2+}$  ions while pH of the suspension remained relatively unchanged for all  $\text{Ca}^{2+}$  ion concentrations.

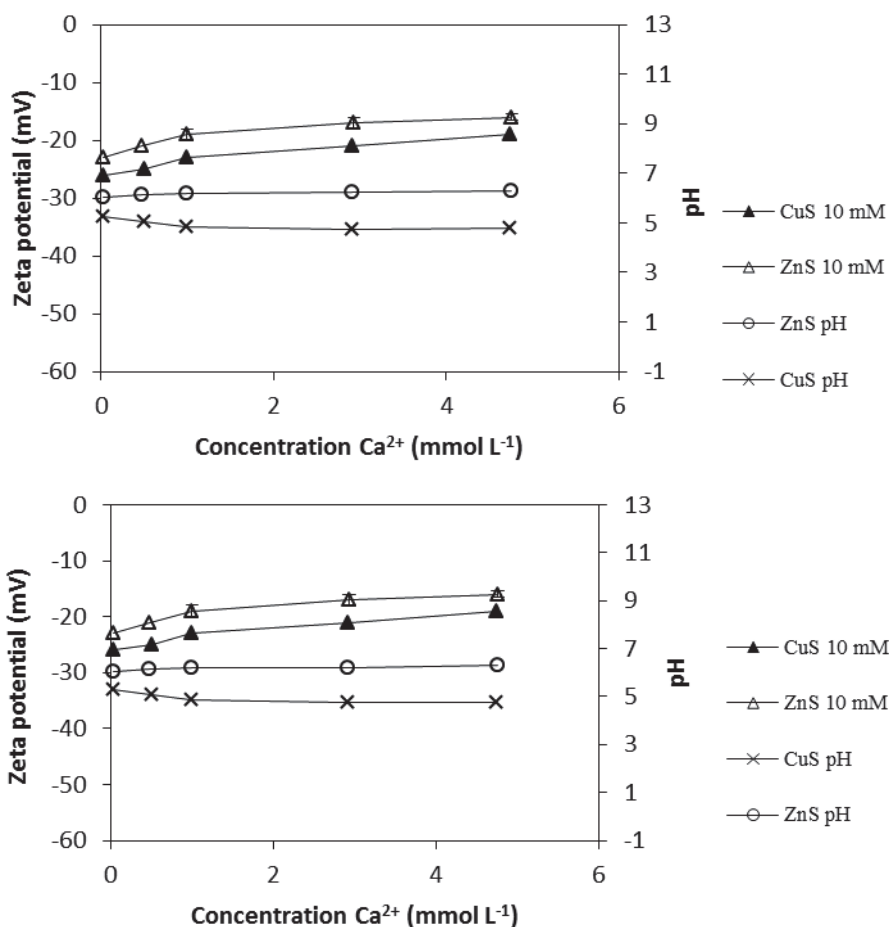


Figure 8.6: Change in zeta potential with cation addition

When aluminium salt is added to aqueous solutions, hydrolysis of  $\text{Al}^{3+}$  ions takes place and different monomeric (i.e.  $\text{Al}(\text{OH})^{2+}$ ,  $\text{Al}(\text{OH})_2^+$ ,  $\text{Al}(\text{OH})_3$ ,  $\text{Al}(\text{OH})_4^-$ ) and polymeric (i.e.  $\text{Al}_2(\text{OH})_2^{4+}$ ,  $\text{Al}_3(\text{OH})_4^{5+}$ ,  $\text{Al}_{13}\text{O}_4(\text{OH})_{24}^{7+}$ ) aqueous complexes are formed (Dentel, 1991). The decrease observed

in the magnitude of the zeta potential of the particles can be attributed to surface adsorption of these complexes on to precipitate particles. In cases where the charge on the surface of the particle was caused by surface adsorbing species, adsorption of  $\text{Al}^{3+}$  ions on the particle surface can occur by formation of complexes between aluminium and surface hydroxyl groups of the particle, i.e. surface complexation (Duan and Gregory, 1996). If the pH of the suspension favours aluminium hydroxide formation, the charged particle surface may be enmeshed into a growing aluminium hydroxide particle (Dentel, 1991). This suggests that the change in zeta potential and suspension pH when  $\text{Al}^{3+}$  ions were added can be attributed to surface adsorption of aqueous  $\text{Al}^{3+}$  ions onto the surface of the precipitates. Adsorption of aqueous  $\text{Al}^{3+}$  ions onto the surface of the precipitate was achieved through surface complexation.

The slight increase observed when the concentration of  $\text{Ca}^{2+}$  ions was increased can be attributed to surface adsorption of these positively charged ions on the precipitate surfaces. Moignard and co-workers (1977) studied the uptake of  $\text{Ca}^{2+}$  ions by zinc sulphide and found that the uptake was directly proportional to pH. The study also found that the adsorption of  $\text{Ca}^{2+}$  ions on the  $\text{ZnS}/\text{H}_2\text{O}$  interface involved the diffusion of the calcium ions into the Stern layer without the release of an equivalent number of protons. Hence, the pH remained relatively unchanged when the  $\text{Ca}^{2+}$  ions were added to the precipitate suspensions. The difference in results obtained between the two ions is consistent with the Schulze-Hardy rule, which states that the ion that causes a dispersion to coagulate is opposite in sign to the electric charge of the colloidal particle and the coagulating power increases with valency of the ion (Stumm, 1992).

### 8.3. Conclusions

Surface properties of particles produced by sulphide precipitation reactions were found to be influenced by suspension pH, ionic strength, excess sulphide concentration and cation addition. An increase in suspension pH, from pH 6 to pH 11, resulted in zeta potential for both copper and zinc precipitates becoming more negative. The magnitude of change was generally greater in the case of zinc, but this was reduced when a high background electrolyte concentration was used because of electrical double layer compression. The point of zero charge for zinc sulphide was found to be around pH 3.5 while reducing the pH to below 7 had little effect on the zeta potential, which remained between -25 mV and -30 mV.

With addition of sulphide to the zinc precipitate suspension, the magnitude of the negative zeta potential was reduced by -10 mV ( from -50 to -40 mV) when 100 mM background electrolyte was used. In the case of copper, addition of a small amount of sulphide resulted in a slight decrease in zeta potential and an increase in mean particle size and surface area and no further change was observed with additional sulphide addition. Charged sulphide species ( $\text{HS}^-$  and  $\text{S}^{2-}$ ) were noted as Potential Determining Ions and were attached on to particle surfaces by adsorption.

The addition of  $\text{Ca}^{2+}$  to both suspensions had little effect on the zeta potential of particles. However, addition of a small amount (0.5 mM) of  $\text{Al}^{3+}$  ions to the copper and zinc precipitate suspensions had a significant effect on the zeta potential of the particles. The zeta potential for zinc particles changed from -23 mV to -5 mV while that for copper particles changed from -28 mV to -10 mV. According to the DVLO theory, these values of zeta potential would promote aggregation of colloid particles and enhance settling.

These results highlight the interventions that can be used to manipulate the charge of particles, post-precipitation, to enhance particle flocculation and precipitate recovery if the conditions under which the precipitates are produced cannot be adequately managed. In the event that supersaturation cannot be controlled, it may be possible to modify the settling characteristics of the precipitant material by using additives that promote coagulation.

## 9. Potential factors affecting solid-liquid separation

### 9.1. Background and objective

Particle surface charge has been shown to depend on various factors that include solution chemistry and nature of surface functional groups (Bebie et al., 1997). In an aqueous based electrolyte the exposed metal ions are strongly hydrated, as are solution cations. The sulphide ions, being highly negatively charged, are strongly bound to available protons from solution and to a lesser extent surrounding water molecules. Consequently, the surface of a sulphide particle is covered with  $-\text{SOH}_2$ ,  $-\text{SOH}$  and  $-\text{SH}$  groups as shown in Figure 9.1 (Bebie et al., 1997). The net charge of the particle depends on the formal charge of each group and the degree of protonation. Work by Fornasiero and co-workers (1992) on pyrite, sphalerite (Healy and Moignard, 1976) chalcopyrite and galena (Kelebek and Smith, 1989) has shown that zeta potential of non-oxidised metal sulphides is highly negative and comparable to that of elemental sulphur.

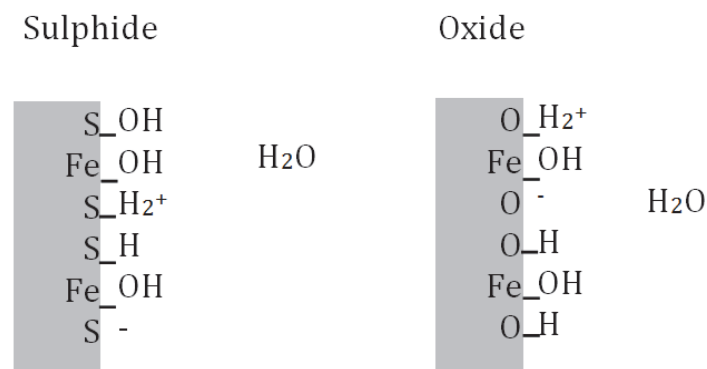
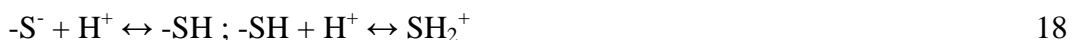


**Figure 9.1: Surface structure of sulphides and oxides (Bebie et al., 1997)**

Raman spectroscopy performed on the surface of sphalerite by Gard and co-workers (1995), confirmed the existence of the  $-\text{SH}$  group. The dependence of zeta potential with pH is largely due to the dissociation of this species and can be illustrated according to Equation 18. At low pH, surface sulphide is fully protonated and as pH increases so does proton dissociation, consequently the particle surface becomes relatively more negative.



On the other hand the surfaces of the corresponding metal oxides are positively charged and the associated surface groups are shown in Figure 9.1. Upon oxidation, the surface of sulphide particles becomes increasingly covered with an oxide/hydroxide layer and this lowers the negative charge on the sulphide particles at the corresponding pH values. The proposed initial oxidation step of metal sulphides is shown by Equation 19, as proposed by Fullston and co-workers (1999). At low pH values the dominant oxidation product is the oxide although there may be subsequent metal dissolution. According to calculations by Fullston and co-workers (1999), the hydroxide group is only thermally stable at pH values greater than 6.



The isoelectric points (IEP) of different metal sulphides in aqueous solution. The majority of authors report an average IEP of less than 2.5 for the respective Fe, Co, Ni, Cu, Zn and Pb sulphides. Consequently, as stated before, sulphide particles in solution exhibit highly negative surface charge at pH values around neutral and higher (Fornaserio et al., 1992, Fullston et al., 1999).

**Table 9.1: IEP of selected metal sulphides**

<b>Formula</b>	<b>Material</b>	<b>IEP</b>	<b>Reference</b>
<b>FeS<sub>2</sub></b>	Pyrite	<2	Bebie <i>et al.</i> , 1998
<b>FeS<sub>2</sub></b>	Pyrite	1.2	Fornaserio <i>et al.</i> , 1992
<b>CoS<sub>2</sub></b>		<2	Bebie <i>et al.</i> , 1998
<b>NiS<sub>2</sub></b>	Vaesite	<2	Bebie <i>et al.</i> , 1998
<b>CuS</b>	Covellite	<1	Liu and Huang, 1992
<b>CuS</b>	Covellite	<2	Mokone <i>et al.</i> , 2010
<b>ZnS</b>	Sphalerite	2.5	Zhang <i>et al.</i> , 1995
<b>PbS</b>	Galena	2.5	Healy and Moignard, 1976

Conversely, the IEP of copper oxide/hydroxide is found at pH values closer to 9.5 (Parks, 1965). In the case of covellite, upon oxidation, the IEP should shift from a value less than 1 and approach that of the oxide. According to Healy and Moignard (1976), the IEP of a metal sulphide gives a good indication of surface oxidation depending on where it lies between that of a pure sulphide and a pure oxide.

The current investigation involved modification of the colloid-surface by partial oxidation of the metal sulphide particles, to this effect oxygen is considered as the additive. In work conducted by Mokone and co-workers (2010), the authors explained the failure of the CuS particles to settle by the relatively high absolute value of their zeta potential, which was found to be between about -30 mV to -45 mV. In the same study zinc sulphide was found to settle and aggregate if precipitated under equi-molar metal to sulphide ratio and as such the effect of oxidation on zinc sulphide particles to aid settling has not been fully explored in this investigation. Partial oxidation of copper sulphide particles should reduce their zeta potential, which will in-turn promote aggregation. Excessive oxidation would however be detrimental, as it results in possible dissolution of metal ions. By carefully controlling the extent to which oxidation on the sulphide particles is permitted it should be possible to shift the isoelectric point of the sulphide colloidal particles and thus promote and improve the settling properties.

## **9.2. Materials and Methods**

### **9.2.1. Reagents**

All the reagents used are as listed in Section 6.2.1.

### **9.2.2. Experimental Design**

The investigation was divided into two phases. The first part of the investigation focused on production of precipitant particles by sulphide precipitation, at a pH of 6 and equi-molar metal to sulphide concentrations. The second part involved partial oxidation of the particles formed at pH 6, with oxygen as the oxidising agent at constant pH. The extent of oxidation was controlled by

limiting the supply of oxygen to the reactor. Characterisation for this part of the experiment was done by zeta potential and metal ion dissolution, all before and after oxidation. Post oxidation, the particles were immersed in solutions of different pH values and the resultant zeta potential noted. The investigation of partial oxidation on the zinc sulphide particles did not include metal dissolution experiments.

### 9.2.3. Experimental Procedure

All precipitation experiments were conducted in a 1.0 L reaction vessel, with a working volume of 0.9 L. The reactor was operated as a CSTR, equipped with 4 baffles and an overhead Rushton turbine run at 600 rpm. The reactor lid had ports for a pH electrode, REDOX probe, nitrogen sparger, reagent inlet and impeller shaft. The reagents were pumped into the reactor using Watson Marlow 520S (Falmouth, UK) pumps at a volumetric flow-rate of  $50 \text{ mL}\cdot\text{min}^{-1}$  per each reagent. Reactor pH was controlled by dosing either 1.0 M HCl or 1.0 M NaOH using a Metrohm auto-titrant (800 Dosino, Switzerland). The dosing device was connected to a computer equipped with control software (Tiamo version 1.2, Metrohm AG, Switzerland).

The oxidation experiments were performed in a 1.0 L batch reactor fitted with 4 baffles and a lid with ports for a redox probe, pH probe, overhead Rushton turbine and a sparger. The oxygen used was of medical grade and controlled at a flow rate of  $30 \text{ cm}^3 \text{ min}^{-1}$ , delivered in to the reactor via a sparger. Agitation was achieved using an overhead stirrer run at 300 rpm to avoid severe attrition.

The particles obtained after oxidation were used for pH-zeta potential analysis with KCl being used as the background electrolyte to adjust ionic strength. The particles withdrawn from the oxidation reactor at 50 min were used for this analysis.

### 9.2.4. Sampling and analytical methods

The generation of colloidal particles in a precipitation reactor depends on several processes that include the chemical reaction, crystallization and mixing. Interaction between these processes generally results in the formation of zones within the working volume of the reactor. The multiple zones exhibit different mixing and supersaturation conditions resulting in different precipitation and reaction conditions, consequently leading to the formation of particles with very different characteristics, e.g. surface properties. To this effect representative sampling and analysis of all the particles remains a challenge. In line with the objective of this study, only particles that did not settle after sample collection during the precipitation step of this investigation were the subject of this investigation. The Malvern zeta sizer nano was used to measure the zeta potential of the particles before and after oxidation.

## 9.3. Results

Upon completion of the copper sulphide precipitation, the formed particles were found to have a zeta potential of about -45 mV with the concentration of residual copper in solution being 9 ppm. The results of change in zeta potential of copper sulphide particles with time, under oxidising conditions are shown in Figure 9.1. The zeta potential of the partially oxidised particles increased between 0 minutes and 20 minutes, after which a sudden reduction in zeta potential was noted at 30 minutes. With increasing time of oxidation, the zeta potential increased until after about 60 minutes, two charge profiles are noted as illustrated in Figure 9.1.

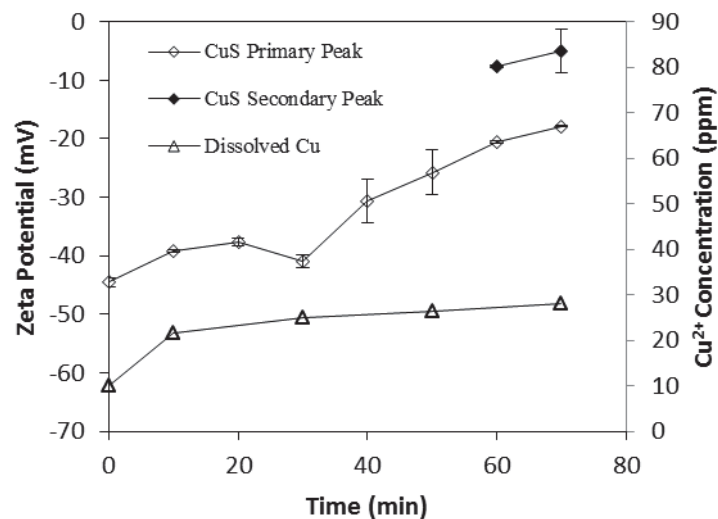


**Figure 9.1: Effect of oxidation on zeta potential of CuS (Concentration right axis, zeta potential left axis)**

A portion of the particle population has a zeta potential of about -20 mV while the rest of the particles are at least 11 mV higher, as shown by the secondary peak in Figure 9.1. After 70 minutes under oxidising conditions, particles with the highest charge have a zeta potential of about -5 mV while those with a lesser charge have a zeta potential of about -18 mV. The concentration of dissolved copper gradually increases up to about 28 ppm at 70 minutes and the total dissolution of copper attributable to oxidation is about 18 ppm.

Post oxidation, the results of the change in zeta potential with pH are shown in Figure 9.2. Immediately after oxidation the zeta potential of the particles was around -22 mV and solution pH was 6. As the solution pH was lowered the zeta potential increased sharply to a maximum of -8.1 mV. A further decrease in pH led to a reversal in the direction of change for the particle zeta potential. At a pH of 3 the zeta potential decreased to -13 mV and a pH of 2 this decreased to around -22 mV.

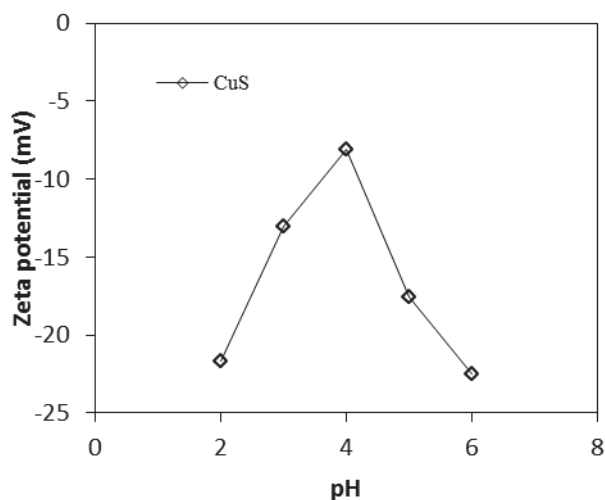


**Figure 9.2: Change in zeta potential of CuS with pH**

The zeta potential of zinc sulphide particles, post precipitation, that have undergone partial oxidation is shown in Figure 9.3. At time 0, which corresponds to non-oxidising conditions, the zeta potential of the zinc sulphide particles was about -22 mV. After 10 minutes the zeta potential of the zinc sulphide particles sharply increased to about -12 mV. This rise became gradual from 10 min to 20 min, with a respective zeta potential change of about 2 mV. After 30 min the zeta potential rose to about -8 mV.

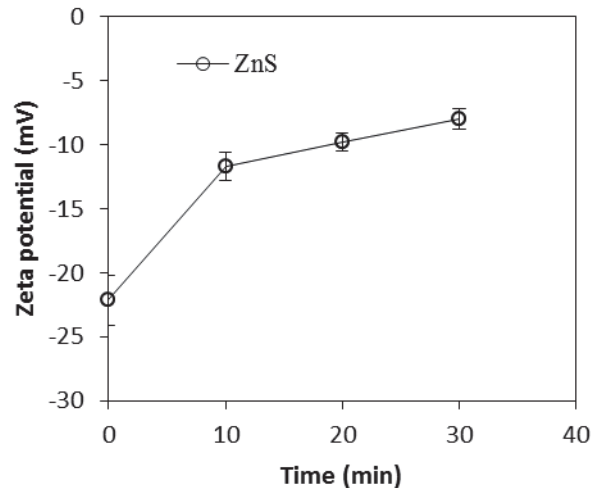


**Figure 9.3: Effect of oxidation on zeta potential of ZnS particles**

#### 9.4. Discussion

The surface of sulphide minerals is highly reactive and if no particular precaution is taken it begins to oxidise as soon as the mineral is in contact with water. This would suggest that, for sulphide oxidation in aqueous solution, the rate limiting step is the mass transfer of oxygen into solution. As oxygen is sparged into the system, oxidation at the surface of the colloid particles immediately commences and begins to cover the surface of the sulphide particles. Healy and Moignard (1976) found that the zeta potential of sulphide particles with respect to pH gives a good indication of oxidation. The oxidation of the copper sulphide particles was carried out at a pH of 6.0 - 6.5 and as oxidation progressed, the relative zeta potential increased, indicating an increase in surface coverage of the sulphide surface with an oxide layer. After 30 minutes of sparging oxygen into the system, a drop in zeta potential was noted. The charge distribution of the particles was fairly narrow, as indicated by the small error bars. This suggests that the withdrawn samples were consistent and of similar characteristics and properties. According to Myerson (2002), due to non-ideal mixing, a crystallizer will develop sub-volumes. These are regions that experience similar conditions of supersaturation, pH and flow and hydrodynamic profiles and the difference between one sub-volume to another may be minimal or relatively large. The consistency of the particles sampled after 30 minutes seems to suggest particles withdrawn from a region of the reactor experiencing low oxygen concentration. As the residence time of the sulphide particles increased, oxidation, as determined by zeta potential increased. After 40 minutes the charge distribution widened, and this is shown by the increase in the size of the error bars. This entails different surface coverage of the sulphide particles with an oxide layer. This could be a consequence of particles oxidising at different rates. Work carried out by Bebie and co-workers (1997), suggests that, for smaller particles, complete surface coverage by an oxide layer is achieved before that of a larger particle. Under the same oxidising conditions the charge on smaller particles will approach zero before that of the larger particles and, with an increment in time, the charge distribution becomes

wider. The same phenomenon was recorded after 50 minutes, but, as the deviation increased, two distinct charge peaks were measured at the 60 and 70 minute mark. The concentration of copper ions in solution increased from about 9 ppm to about 28 ppm, indicating metal sulphide dissolution.

When the pH of the particles produced after 50 min of oxidation was decreased from 6.0 to 5.0 the zeta potential of the particles increased from -22.5 mV to -18 mV. This is consistent with protonation of the remaining sulphide surface sites, resulting in a reduced negative charge. With an increase in hydrogen ion concentration, the particle charge should approach zero as protonation increases and less exposed sulphide sites remain. This trend was generally observed down to a pH of 4, at which point the zeta potential of the particles attained a local maximum and began to decline as the pH decreased further. This is due to the dissolution of the oxide layer according to the solubility properties of copper oxide in an acidic medium. Fullston and co-workers (1999) observed this trend for copper sulphide minerals with the exception of chalcocite. Resistance to dissolution was attributed to a more tenacious oxide layer on the chalcocite. Due to dissolution, a measure of the IEP post oxidation becomes difficult because the colloid particles revert to their sulphide surface at low pH values. The IEP values stated in Table 9.1 for pristine copper sulphide surfaces are associated with a zeta potential value of about -20 mV at a pH of 4, which compares with that of oxidised copper sulphide in this investigation of about -8 mV. This extrapolates to an IEP of the oxidised sulphide to be between a pH of 3 and 4 if dissolution were not to have taken place.

The effect of oxidation on the zinc sulphide system was consistent with that of the copper sulphide system. As partial oxidation of the surface increased, the zeta potential of the respective particles also increased. However, as compared to the copper sulphide system, the zinc sulphide particles attained a zeta potential less than -10 mV in only 30 minutes while for copper sulphide such a charge was attained after at least 60 minutes. This is most likely due to different starting zeta potentials for the respective metal sulphides produced under inert conditions, copper sulphide particles at time 0 had a zeta potential of about -45 mV while the respective zinc sulphide particles had a zeta potential of -22 mV.

## **9.5. Conclusions**

It is proposed that modification of the surfaces of metal sulphide particles could be used to decrease their negative zeta potential and thus improve their settling properties. This work has shown that surface modification by partially oxidising metal sulphide particles is possible. Partial oxidation of the sulphide particles has shown an associated increase in zeta potential, for copper sulphide particles this is from about -45 mV to at least -18 mV, after 70 min under oxygen and for zinc sulphide this is from about -23 mV to about -8 mV. Since dissolution has been observed, the residence time of the sulphide particles has to be carefully controlled to avoid unsustainable levels of metal ion dissolution. At near neutral pH and above, dissolution should be fairly inhibited. It can be inferred that the IEP of oxidised copper sulphide particles lies between a pH of 3 and 4, a respective increase from the reported pH of less than 2 as shown in Figure 9.2.

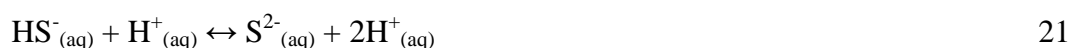
## 10. Investigation of using FeS Slurry as a slow release sulphide source

### 10.1. Background

Various methods have been used on different metal sulphide systems to try and reduce the particle electrostatic repulsion (zeta potential) in order to induce settling. The methods involved include the control of supersaturation to produce non colloidal particles, by promotion of growth and secondary nucleation (Sampaio et al., 2010), as well as the use of additives which may promote coagulation (Mokone et al., 2012). Some of these techniques have already been explored and discussed in this report and may be considered successful to varying extents.

It has become generally accepted that the prerequisite for the production of non-colloidal sulphide particles is to operate under mildly supersaturated conditions (Jones et al., 1996; van Hille et al., 2005). Several mechanisms to control supersaturation have been proposed, some of which have been reviewed in this report. Among these processes, Hammack and co-workers (1993) successfully exploited the pH dependence of sulphide speciation as well as the mass transfer resistance in controlling supersaturation. They operated a hydrogen sulphide-based precipitation process under acidic conditions. This reduced the rate of  $\text{H}_2\text{S}_{(g)}$  dissolution, thereby reducing the equilibrium concentration of the  $\text{HS}^-$  ion in solution resulting in a decrease in the effective supersaturation. A notable decrease in the amount of fines produced was reportedly observed. The equilibrium relationship that exists between the species:  $\text{H}_2\text{S}_{(aq)}$ ,  $\text{HS}^-$  and  $\text{S}^{2-}$  is as defined by Figure 10.1 (Lewis 2010).

Karbanee and co-workers (2008) also exploited mass transfer resistance, from the dissolution of sparged  $\text{H}_2\text{S}_{(g)}$ , to control sulphide dosing. Although the method managed to successfully control sulphide ion dosing, the process was compromised by the production of  $\text{H}^+$  ions as a result of  $\text{H}_2\text{S}$  decomposition as defined in Equations 20 and 21:



The hydrogen ions lowered the pH to levels that promoted the dominant speciation of  $\text{H}_2\text{S}_{(aq)}$  in solution over that of the  $\text{HS}^-$  and  $\text{S}^{2-}$  ions as shown in Figure 10.1. To prevent the exhaustion of the  $\text{HS}^-$  ion in solution, NaOH had to be continually added as a pH modifier to raise the pH and maintain optimal  $\text{HS}^-$  speciation.

The use of  $\text{H}_2\text{S}_{(g)}$  as means of sulphide precipitation has clearly shown potential in reducing the effective supersaturation for precipitation processes, however, it also has several challenges which may render the overall process unsustainable and hazardous. Such challenges include the need to continually add pH modifiers in order to maintain optimal  $\text{HS}^-$  speciation. Hydrogen sulphide gas which is the source of sulphide ions is also highly toxic and its use may increase the complexity of the precipitation set-up and equipment due to introduction of the necessary safety measures. As such, it may be necessary to explore other supersaturation controlling techniques.

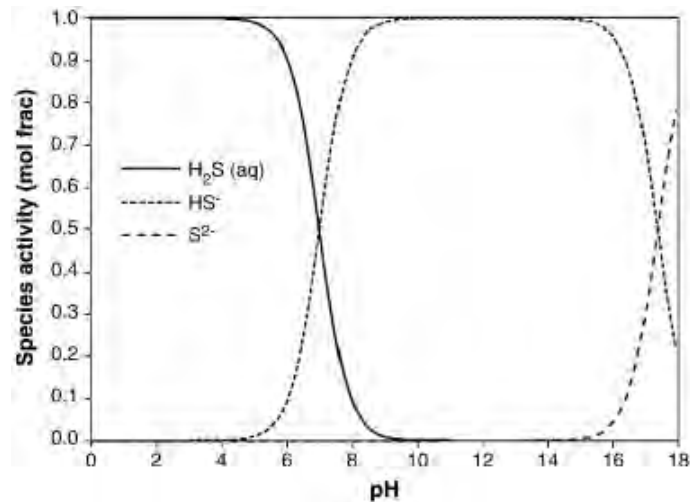


**Figure 10.1: pH dependence of hydrogen sulphide speciation (Lewis, 2010)**

According to Schlauch (1978), non-colloidal metal sulphide particles can be formed by controlled sulphide release into a solution containing pollutant metal ions. He proposed the addition of a metal sulphide slurry, such as FeS, having a higher solubility into a stream containing metal ions, such as Cu<sup>2+</sup> ions, with a much lower metal sulphide solubility. When the FeS slurry is added to the Cu<sup>2+</sup> metal ion stream it attains equilibrium according to Equation 22 and is governed by the equilibrium solubility product. Due to a much lower solubility product of CuS, all available S<sup>2-</sup> ions react with Cu<sup>2+</sup> ions according to Equation 23 and precipitate CuS. As Equation 23 consumes S<sup>2-</sup> ions, the equilibrium of Equation 22 shifts to the right resulting in further dissolution of FeS into its constituent ions. The process of CuS precipitation thus becomes controlled by the dissolution of FeS, which is dependent on pH, temperature and solids concentration. Although this process may seem viable it depends greatly on the ability to isolate a pure metal sulphide, to be used as a sulphide ion source.



### 10.1.1. Choice of precipitating agent

Any metal ion which has a higher equilibrium sulphide concentration than the sulphide of the metal pollutants in a metal ion rich stream can be used to form a sulphide slurry that acts as a sulphide source (Schlauch, 1978). This means that according to Table 10.1, MnS can be used as a sulphide source for precipitating all the subsequent metal ions as sulphides. The selection process can then be further influenced by cost and availability of the metal salt. For the purpose of this investigation, FeS will be used as a sulphide source, as it is less expensive and more abundant in acid mine drainage than MnS. According to the theory of sulphide dissolution the least driving force with regard to FeS dissolution will be experienced when Zn<sup>2+</sup> ions are used as the pollutant ions while the largest driving force will be experienced when Cu<sup>2+</sup> ions the pollutant ions. This is largely influenced by the difference in the respective equilibrium solubility constants.

**Table 10.1: Metal sulphide equilibrium  $k_{sp}$  values at 18°C (Schlauch, 1978)**

Metal Ion	Equilibrium Sulphide Concentration at 18°C (mol/L)
Mn <sup>2+</sup>	$3.75 \times 10^{-8}$
Fe <sup>2+</sup>	$6.1 \times 10^{-10}$
Zn <sup>2+</sup>	$3.46 \times 10^{-12}$
Ni <sup>2+</sup>	$1.18 \times 10^{-12}$
Sn <sup>2+</sup>	$3.1 \times 10^{-13}$
Co <sup>2+</sup>	$1.73 \times 10^{-13}$
Pb <sup>2+</sup>	$1.84 \times 10^{-14}$
Cu <sup>2+</sup>	$9.2 \times 10^{-23}$

### 10.1.2. Operating conditions

While much research has been conducted on the solubility of FeS at room temperature, very few researchers investigated the dependence of the solubility of FeS on temperature. Benning and co-workers (2000) suggested Equation 24 to calculate the solubility limit as a function of temperature.

$$K_{sp,a} = 10^{\left(\frac{2848.8}{T_K} - 6.347\right)} \quad 24$$

With regards to the effect of pH on the solubility of FeS, Rickard (2006) showed that the following equation can be used to describe the relationship at 23°C between a pH of 3 and 10:

$$\log[\text{Fe(II)}]_T = \log K_0[\text{FeS}_m] + \log K_{1,sp}^+ - \log[\text{H}_2\text{S}] - 2\text{pH} \quad 25$$

where [Fe(II)]<sub>T</sub> represents the total dissolved Fe<sup>2+</sup> concentration,  $\log K_0[\text{FeS}_m] = -5.7$  and  $\log K_{1,sp}^+ = 3.5 \pm 0.25$  for the pH dependent reaction of FeS dissolving into its constituent ions of Fe<sup>2+</sup> and S<sup>2-</sup>. However, another way in which the solubility of FeS with respect to pH can be determined is by modelling the solid percentage of FeS versus pH. This was done on Visual Minteq and the results are shown in Figure 10.2.

As shown in Figure 10.2, the minimum concentration of lattice ions in a solution that is in equilibrium with FeS solid can be attained at pH levels greater than 8. In contrast, the results also show that the maximum concentration of dissolved lattice ions in equilibrium with solid FeS can be attained at pH values of 5 and lower. Consequently, the rate of FeS dissolution can be increased or decreased by changing pH between the upper and lower pH values of 8 and 5 respectively.

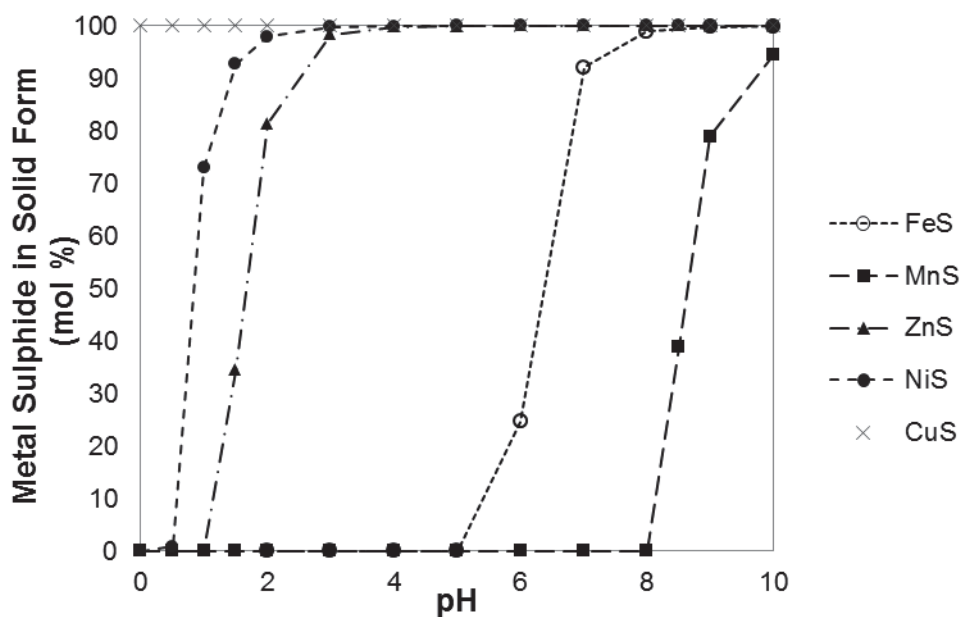


Figure 10.2: MeS solids percentage versus pH at 25°C obtained from Visual minteq

## 10.2. Scope of investigation

The investigated method of sulphide release was proposed as a potential sulphide source for the precipitation of metal ions from large water volumes. In this regard, changing the temperature as a means of controlling FeS dissolution was deemed as being energetically expensive and unsustainable hence it was not explored in the current investigation. Firstly, the effect of pH on the dissolution of FeS was investigated with respect to dissolved  $\text{Fe}^{2+}$  ion concentration then with respect to the concentration of the dissolved pollutant ions.

## 10.3. Materials and Methods

### 10.3.1. Experimental Design

The investigation was divided into two phases, the first being the production of an FeS slurry and then the second phase being the dissolution of FeS and the simultaneous precipitation of the pollutant metal ions. All the experiments were carried out at room temperature (25°C) and standard pressure.

### 10.3.2. Reagents

The following reagents were used in this investigation:  $\text{FeSO}_4 \cdot 7\text{H}_2\text{O}$ ,  $\text{ZnSO}_4 \cdot 7\text{H}_2\text{O}$ ,  $\text{Na}_2\text{S} \cdot 9\text{H}_2\text{O}$ , NaOH, HCl and gaseous nitrogen. All the chemicals used were of analytical grade obtained from Sigma Aldrich and used without further purification. The nitrogen used was obtained from Afrox South Africa in a 200 bar cylinder which was regulated to standard pressure during use.

### 10.3.3. Experimental set-up

The reactor used in this investigation consists of a 2 litre batch reactor fitted with a lid and four baffles. Mixing in the reactor was achieved by a Rushton turbine connected to an overhead stirrer with variable RPM. The impeller used had four pitched blades with a 5.6 cm diameter. Control of

pH in the reactor was achieved by the automatic dosing of either 0.5 M HCl or 0.5 M NaOH using the Metrohm 800 Dosino autodosing unit. The lid of the reactor had six ports to cater for a pH electrode, sulphide probe, turbine impeller shaft, nitrogen gas inlet, reagent inlet and an acid/base injection nozzle. Metal and sulphide reagents were pumped into the reactor using pre-calibrated Watson Marlow 520S (Falmouth, UK) pumps.

### 10.3.4. Analytical Techniques

The primary analytical technique in this investigation involved measurement of the dissolved metal ion concentration. This was done using Inductively Coupled Plasma Optical Emission Spectrometry analysis (ICP-OES). All solutions were filtered through a nylon filter paper with a pore size of 0.20  $\mu\text{m}$  before analysis.

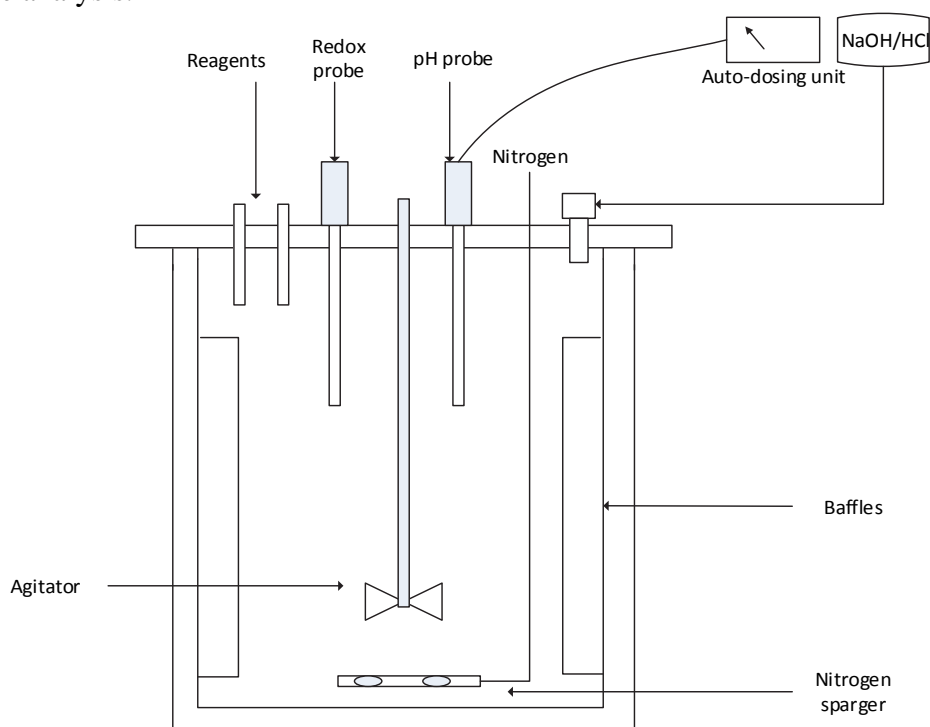


**Figure 10.3: Batch reactor used for the precipitation of FeS**

## 10.4. Experimental Procedures

### 10.4.1. Precipitation of FeS

Water de-oxygenation was achieved prior to solution preparation by boiling the de-ionised water for at least 10 minutes then allowing it cool in a closed container. During solution preparation, oxygen contamination was avoided by sparging nitrogen whenever the vessel containing the solution was open to the atmosphere. A solution of  $\text{Fe}^{2+}$  ions was made up to a concentration of  $1000 \text{ mg.L}^{-1}$  and a  $\text{S}^{2-}$  ion solution was made equi-molar to this.

The batch reactor was half filled (1 L) with de-ionised water after which the overhead stirrer was switched on and set at 650 rpm. Nitrogen gas was sparged through the reactor for 30 minutes before the reagents were pumped into the reactor simultaneously via the peristaltic pumps. The reagent flowrate was kept constant at  $0.5 \text{ L.min}^{-1}$  throughout the experiment for both the reagents. Oxygen

contamination in the stock solution vessels was prevented by continuous nitrogen sparging and the pH was kept at 6. Reagent dosing into the reactor was stopped after a combined reagent delivery of 1 L into the reactor. The contents of the reactor were left for an hour under agitation and then a further hour without agitation to aid settling. All the supernatant was decanted out of the vessel and then the remaining suspension was placed in a centrifuge at low RPM for 30 min. The FeS particles were then collected in an air tight vessel together with a minimal amount of the mother liquor solution to form the FeS slurry.

#### **10.4.2. Investigation of FeS dissolution**

After production of the FeS slurry, all the solid material produced was placed in a litre of de-oxygenated de-ionised water and then agitated for 20 min at 350 rpm under nitrogen. This experiment was only conducted for 20 minutes because this was the period deemed to be consistent with conditions representing a solution in which sulphide ions are continually consumed as the dissolution of FeS progresses. Longer periods of dissolution would result in a decrease in the driving force of dissolution due to a lower concentration gradient. This is because all the dissolved sulphide ions are not consumed once in solution as no pollutant ions are present. Samples were withdrawn from the holding vessel over the duration of the dissolution experiment in order to analyse the  $\text{Fe}^{2+}$  ion concentration.

#### **10.4.3. Precipitation of pollutant metal ions**

The concentration of the pollutant metal ions was kept at a constant concentration of  $200 \text{ mg.L}^{-1}$ . A stream of zinc ions was used in this investigation as it represented the worst case scenario in terms of being the next least soluble metal sulphide from FeS. This was based from the understanding that if the proposed method works for ZnS precipitation then it would work for all the subsequent metal sulphide systems that possess a much lower solubility product. In order to create a large enough driving force for the dissolution of FeS, all the FeS slurry produced in the 2 L batch reactor was collected and placed in a litre of solution containing the  $\text{Zn}^{2+}$  ions. The combined slurry pollutant mixture was sparged with nitrogen and agitated with a Rushton turbine at 350 revolutions per minute and then allowed to react for 650 minutes. In order to measure the dissolution of FeS and simultaneous precipitation of ZnS, samples were withdrawn from the reacting vessel at regular intervals and analysed for metal ion concentration via ICP OES analysis.

### **10.5. Results**

The results of the investigation into the dissolution of FeS at various pH values and ambient temperature are shown in Figure 10.4. Although all possible attempts were made at keeping the dissolution pH at values of 6, 7 and 8 slight deviations were unavoidable and the actual pH values are shown in the legend of Figure 10.4. The results are based on the dissolution of FeS in distilled water.

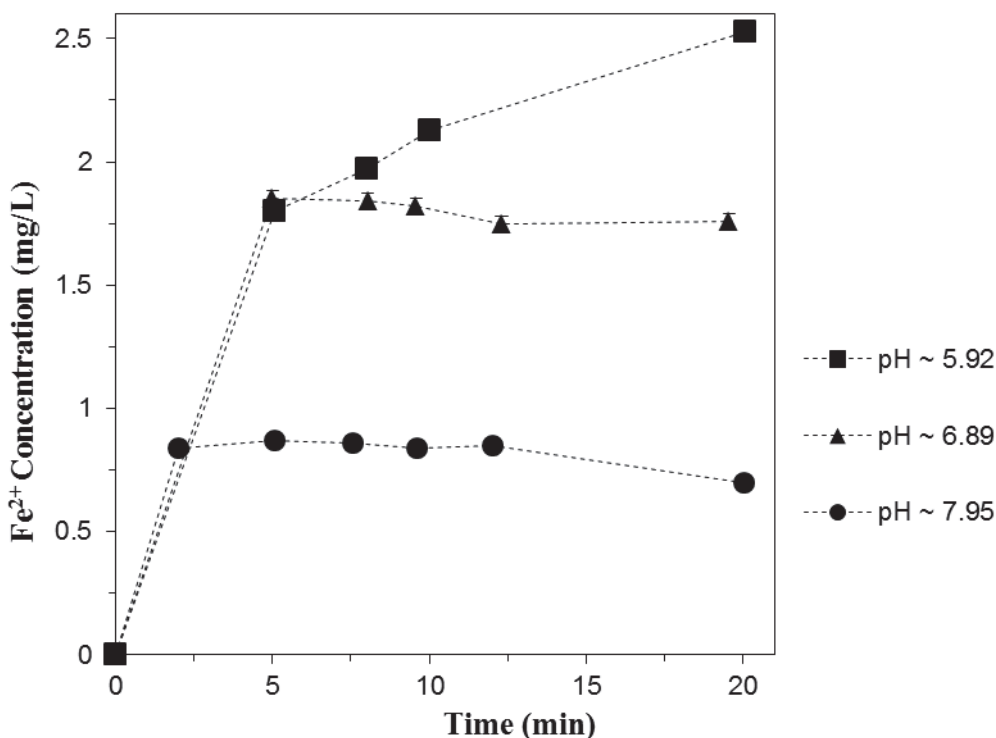


**Figure 10.4: Effect of pH on the concentration of ferrous ions in solution with time**

The general trend shown in Figure 10.4 shows a decrease in dissolved  $\text{Fe}^{2+}$  ions with an increase in pH. A maximum  $\text{Fe}^{2+}$  ion concentration of  $2.53 \text{ mg.L}^{-1}$  was achieved after 20 min at a pH of 5.92 while the least  $\text{Fe}^{2+}$  ion concentration of  $0.7 \text{ mg.L}^{-1}$  after 20 min was achieved at a pH of 7.95. The intermediate pH of 6.89 resulted in an intermediate  $\text{Fe}^{2+}$  ion concentration of  $1.76 \text{ mg.L}^{-1}$ . At a pH of 5.92, there was a step rise in the initial concentration of  $\text{Fe}^{2+}$  ions after the first 5 min, beyond this time the rate of metal ion increase with time decreased. For dissolution at a pH of 6.89 there is an initial rise in  $\text{Fe}^{2+}$  ion concentration from 0 to  $1.85 \text{ mg.L}^{-1}$  after the first 5 minute interval, beyond which the concentration became relatively constant. The same trend was observed for the dissolution at a pH of 7.95 although the  $\text{Fe}^{2+}$  ion concentration became relatively constant at a much lower concentration of  $0.84 \text{ mg.L}^{-1}$ .

After the addition of an FeS slurry to a solution of  $\text{Zn}^{2+}$  ions, the concentration of both  $\text{Fe}^{2+}$  and  $\text{Zn}^{2+}$  ions was measured at various time intervals in order to monitor both FeS dissolution and ZnS precipitation. The results of  $\text{Fe}^{2+}$  dissolution with time at a pH of 5.94 are shown in Figure 10.5.

Immediately after the addition of the FeS slurry the concentration of  $\text{Fe}^{2+}$  ions in solution increased to about  $6.9 \text{ mg.L}^{-1}$ . With an increase in time there was a further increase in the concentration of ions up to a concentration of  $8.68 \text{ mg.L}^{-1}$  after which the concentration fluctuates around a concentration of  $8.9 \text{ mg.L}^{-1}$ . The results of the corresponding  $\text{Zn}^{2+}$  ion concentration in solution are shown in Figure 10.6 and they show the change in concentration of  $\text{Zn}^{2+}$  ions with time as FeS dissolved liberating  $\text{S}^{2-}$  ions.

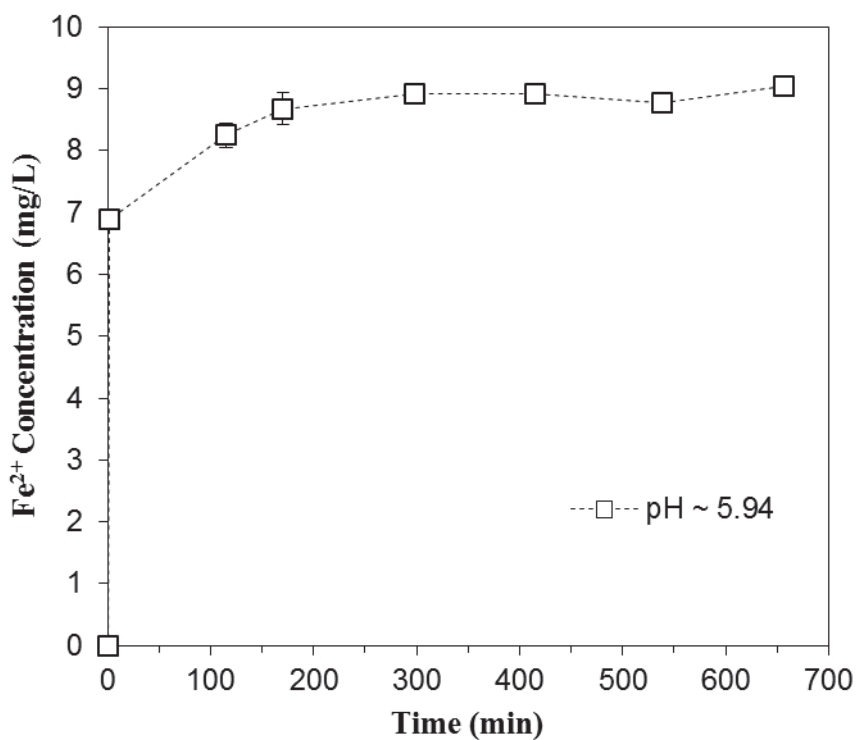


**Figure 10.5: Variation of Fe<sup>2+</sup> ion concentration with time during simultaneous dissolution of FeS and precipitation of ZnS**

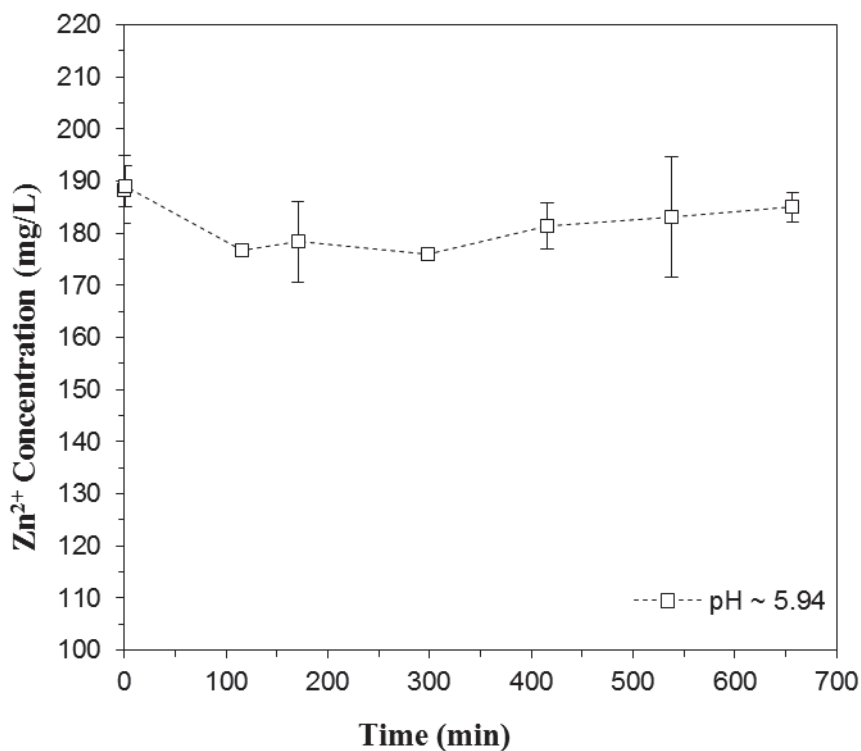


**Figure 10.6: Concentration of Zn<sup>2+</sup> ions in solution during dissolution of FeS**

The initial concentration of the Zn<sup>2+</sup> ions was around 188 mg.L<sup>-1</sup> immediately after the addition of the FeS slurry. This decreased in the first 115 min of the experiment to about 177 mg.L<sup>-1</sup> after which the concentration fluctuated between a maximum of 188 mg.L<sup>-1</sup> and a minimum of 176 mg.L<sup>-1</sup>.

## 10.6. Discussion

The results presented in Figure 10.4 show a trend of increase in the rate of FeS dissolution with a decrease in pH. This is consistent with the results predicted by Visual Minteq. The initial increase in the  $\text{Fe}^{2+}$  ion concentration is observed within the first 5 minutes after the addition of the FeS slurry may not be due to dissolution but to the residual amount of  $\text{Fe}^{2+}$  ions inherent in the mother liquor of the FeS slurry. The much lower initial concentration (within the first 5 min) observed at a pH of 7.95 may be due to a very much lower solubility concentration of ions as predicted by Visual Minteq. The relative consistency in  $\text{Fe}^{2+}$  ion concentration exhibited by dissolution experiments at pH values of 7.95 and 6.89 suggested a minimal driving force for FeS dissolution and as such the current investigation focused on dissolution investigations at a pH of 5.92 (approximately 6), where a significant driving force of FeS to its constituent ions was observed.

As the solid FeS particles dissolved, they liberated both  $\text{S}^{2-}$  ions and  $\text{Fe}^{2+}$  ions, the extent of dissolution was monitored by measuring the concentration of  $\text{Fe}^{2+}$  ions, with time, as the  $\text{S}^{2-}$  were consumed by the free  $\text{Zn}^{2+}$  ions. This means that the increase in the number of moles of  $\text{Fe}^{2+}$  ions in solution should equate to the number of moles of  $\text{Zn}^{2+}$  ions lost from the solution. As shown in Figure 10.5 and 10.6, there was an increase of  $2.14 \text{ mg.L}^{-1}$  of  $\text{Fe}^{2+}$  which translates to  $0.0383 \text{ mM}$  while this corresponded to a decrease in the  $\text{Zn}^{2+}$  ion concentration of  $3 \text{ mg.L}^{-1}$  translating to  $0.0459 \text{ mM}$ . The difference between the moles of zinc precipitated and iron dissolved could mean either of two possibilities. The discrepancy could have arisen due to analytical errors in determining metal ion concentration or it could have arisen due to the precipitation of  $\text{Zn}^{2+}$  ions on the surface of the FeS particles. The latter gives rise to  $\text{Zn}^{2+}$  bonding to uncoordinated sulphide ions on the surface of the FeS particles. This situation results in the decrease of  $\text{Zn}^{2+}$  ions in solution without much FeS dissolution. However, this may result in the encapsulation of the FeS particles leading to a decline in the dissolution rate of FeS. This is also consistent with work by Pankow (1979), indicating that the presence of metal ions inhibited the dissolution of FeS since they may most likely associate with FeS, and form an aggregate of the form  $(\text{MS})_n(\text{FeS})_m$ .

Initial predictions of the current investigation were based on visually distinguishing between the ZnS and FeS particles because of their differences in colour. FeS particles are black while ZnS particles are white to off white. However, with the progression of the experiment no white particles in the solution were observed. In contrast, the FeS particles changed colour to dark brown. Saad (1998) also noted that the ZnS precipitate synthesized through FeS dissolution was a distinct dark brown colour which further alludes to the fact that the ZnS precipitated on the surface of the FeS particles.

## 10.7. Supersaturation reduction

Although the current method did not result in the precipitation of a large amount of ZnS, A comparison was drawn between the supersaturation levels achieved through the use of FeS dissolution and the use of the conventional precipitation method where sulphide and zinc ions in solution are mixed simultaneously. The level of supersaturation was calculated by Equation 2 (Page 3).

The results shown in Figure 10.7 show a reduction in supersaturation by a factor of about 4.4 between conventional precipitation methods and a mass transfer resistance slow sulphide release

technique. This result confirms the findings of Sampaio (2010) and Santheep et al. (2008) who showed that the controlled release of the sulphide ion results in the reduction of supersaturation.

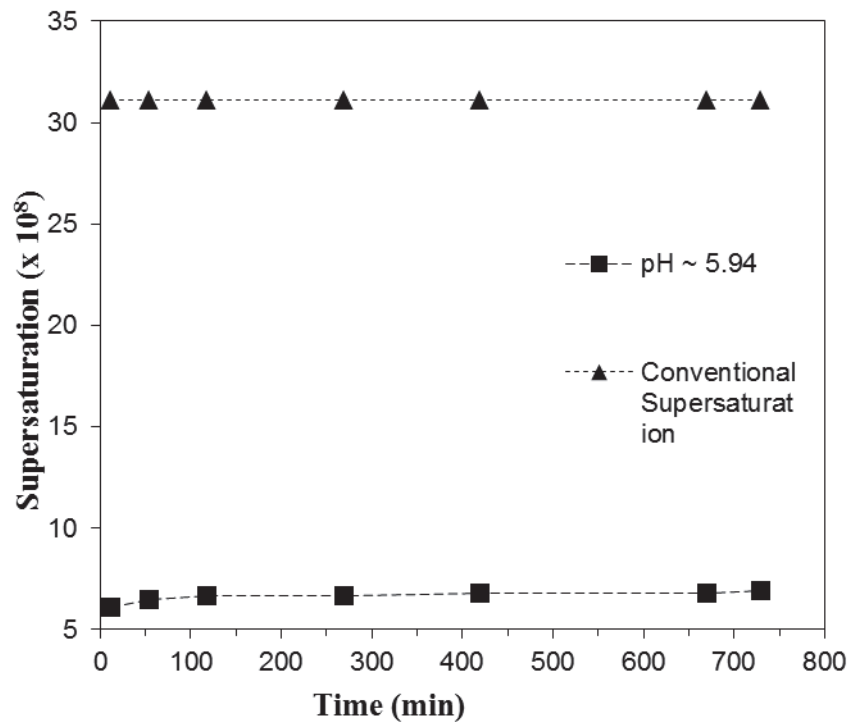


**Figure 10.7: Comparison between the Conventional Supersaturation Level and the Supersaturation Levels Achieved Through the Use of FeS**

## 10.8. Conclusions

The results presented in this investigation have shown that FeS dissolution can be used to control supersaturation by a factor of up to 4.4. Since  $Zn^{2+}$  is the metal ion with the next lowest metal sulphide concentration after  $Fe^{2+}$ , the fact that the concentration of  $Zn^{2+}$  ions was reduced for this “worst case scenario” advocates that this method may be more successful for metal sulphides that have much lower equilibrium solubilities. However, although a much lower solubility may result in an increased driving force for precipitation, it may not necessarily alleviate the challenge of FeS encapsulation.

On the other hand, if surface precipitation of a pollutant metal is specific or prefers certain base metal ions over others then this process could be used as a selective precipitation mechanism from a multi-component metal ion stream. In such a case it may be less complex to deal with two metal sulphide complexes than to deal with a more diverse slurry of base metal sulphide ions.

## **11. Overall conclusions**

The main aim of the research was to further the understanding of the precipitation of metal sulphides in the treatment of acid mine drainage via sulphate reduction and metal precipitation. This was carried out in a four-part investigation.

### **11.1. Studies to investigate effect of reaction conditions on particle characteristics**

Reaction conditions were found to have a significant effect on particle characteristics. An increase in the amount of sulphide ions at a constant metal ion concentration in solution during metal sulphide precipitation resulted in small, highly charged particles with poor settling characteristics. Colloid surface charge was strongly influenced by sulphide ions present in solution and this affected copper sulphide particles to a larger extent than zinc sulphide particles. There is possible selective adsorption of sulphide ions on copper sulphide particles when sulphide is in excess but further investigations need to be carried out to verify this. Aggregation is inhibited when primary metal sulphide particles possess a zeta potential more negative than a certain threshold value. This is consistent with literature findings.

### **11.2. Studies to investigate whether or not there is a specific zeta potential value at which aggregation is suppressed**

The surface properties, and thus the aggregation behaviour, of the metal sulphide particles were found to be influenced by suspension pH, ionic strength, excess sulphide concentration and cation addition. An increase in suspension pH increased the magnitude of zeta potential for both copper and zinc precipitates. The magnitude of increase was generally greater in the case of zinc, but this was reduced when a high background electrolyte concentration was used because of electrical double layer compression.

With addition of sulphide to the suspension, the magnitude of the negative zeta potential was reduced by -10 mV (from -50 to -40 mV when 100 mM background electrolyte was used) in the case of zinc and only slightly in the case of copper. In the case of copper, there was also an increase in mean particle size and surface area. Charged sulphide species ( $\text{HS}^-$  and  $\text{S}^{2-}$ ) were noted as Potential Determining Ions and were attached on to particle surfaces by adsorption.

The addition of  $\text{Ca}^{2+}$  to both suspensions had little effect on the zeta potential of particles. However, the addition 0.5mM of  $\text{Al}^{3+}$  ions to the copper and zinc precipitate suspensions had a significant effect on the zeta potential of the particles. The zeta potential for zinc particles changed from -23 mV to -5 mV while that for copper particles changed from -28 mV to -10 mV. According to the DVLO theory, these values of zeta potential would promote aggregation of colloid particles and enhance settling.

These results highlight the interventions that can be used to manipulate the charge of particles, post-precipitation, to enhance particle flocculation and precipitate recovery if the conditions under which the precipitates are produced cannot be adequately managed.

### **11.3. Potential factors affecting solid-liquid separation**

This part of the investigation showed that surface modification by partially oxidising metal sulphide particles is possible. Partial oxidation of the sulphide particles has shown an associated increase in

zeta potential, for copper sulphide particles this is from about -45 mV to at least -18 mV, after 70 min under oxygen and for zinc sulphide this is from about -23 mV to about -8 mV. Since dissolution has been observed, the residence time of the sulphide particles has to be carefully controlled to avoid unsustainable levels of metal ion dissolution. At near neutral pH and above, dissolution should be fairly inhibited. An inference in this study is made that the IEP of oxidised copper sulphide particles lies between a pH of 3 and 4, which is slightly higher than the value reported in literature.

#### **11.4. Investigation of using FeS Slurry as a slow release sulphide source**

The results presented in this investigation have shown that FeS dissolution can be used to control supersaturation by a factor of up to 4.4. Since  $Zn^{2+}$  is the metal ion with the next lowest metal sulphide concentration after  $Fe^{2+}$ , the fact that the concentration of  $Zn^{2+}$  ions was reduced for this “worst case scenario” suggests that this method may be more successful for metal sulphides that have much lower equilibrium solubilities. However, although a much lower solubility may result in an increased driving force for precipitation, it may not necessarily alleviate the challenge of FeS encapsulation.

On the other hand, if surface precipitation of a pollutant metal is specific or if there is a preference for certain base metal ions over others, then this process could be used as a selective precipitation mechanism from a multi-component metal ion stream. In such a case it may be less complex to deal with two metal sulphide complexes than to deal with a more diverse slurry of base metal sulphide ions.

**In summary, metal sulphide precipitation has shown potential as a method for the removal of metals from industrial pollutant streams. Although its relatively low solubility products and fast reaction kinetics mean that the process has a number of challenges, it is still a superior choice to that of metal hydroxide precipitation.**

The findings of the current work are, firstly, that that metal sulphide particles obey the DLVO theory. However, the reported threshold value for the promotion of aggregation of about -38 mV is difficult to achieve under viable operational conditions. The pH during precipitation either has to be very high, resulting in the need for a high dosage of pH modifiers, or the colloidal suspension has to be treated with significant amounts of coagulants. This reduces the viability of sulphide precipitation as a precipitation method.

This work has also shown that other mechanisms of inducing settling, such as partial oxidation of precipitant material, are effective, but only in synthetic mono-component streams. The consequence of using such a technique for typical industrial multicomponent streams and acid mine drainage is that altering the solution redox not only affects the target material, but may induce catalytic reactions that may transform the precipitant material into an undesired product. Further studies with multicomponent systems would be required.

The last major finding of this work is that using FeS as a slow sulphide release source for the precipitation of lower solubility product metal sulphides suffers from limitations that render it not viable for industrial use. The encapsulation of FeS by ZnS that was observed in the current process inhibited further dissolution of the sulphide source, thus stopping the precipitation process.

It is recommended that future work in this area focus on the production of a metal sulphide product that is easily separable from the industrial waste stream. Two of the most promising contenders for processes are **electrocoagulation** and the application of a **magnetic field** application. Both of these processes have the ability to address the biggest issue with metal sulphide formation – the difficulty of promoting settling - and both of them do so without the addition of any additional reagents.

## 12. References

- ADLER PM (1987) Hydrodynamic properties of fractal flocs. *Faraday Discussions of the Chemical Society* **83** 145-152.
- BEBIE J, SCHOONEN MAA, FUHRMANN M and STRONGIN DR (1998) Surface charge development on transition metal sulfides: An electrokinetic study. *Geochimica et Cosmochimica Acta* **62(4)** 663-642.
- BENNING LG, WILKIN RT and BARNES HL (2000) Reaction pathways in the FeS system below 100°C. *Chemical Geology* **167(1)** 25-51.
- BHATTACHARYYA D and CHEN L (1986) *Sulfide precipitation of nickel and other heavy metals from single- and multi-metal systems*, Cincinnati: Water Engineering Research Laboratory.
- BIJMANS FMM, VAN HELVOORT P-J, BUISMAN CJN and LENS PNL (2009) Effect of the sulfide concentration on zinc bio-precipitation in a single stage sulfidogenic bioreactor at pH 5.5. *Separation and Purification Technology* **69** 243-248.
- BRAMLEY AS and HOUNSLOW MJ (1996) Aggregation during precipitation from solution: A method of extracting rates from experimental data. *Journal of Colloid and interface Science* **1(183)** 155-165.
- BRYSON AW and BIJSTERVELD CH (1991) Kinetics of the precipitation of manganese and cobalt sulphides in the purification of a manganese sulphate electrolyte. *Hydrometallurgy* **27** 75-84.
- CLARKE P, FORNASIERO D, RALSTON J and SMART RSC (1995) A study of the removal of oxidation products from sulphide mineral surfaces. *Minerals Engineering* **8(11)** 1347-1357.
- DEKKERS JM and SCHOONEN MAA (1994.) An electrokinetic study of synthetic greigite and pyrrhotite. *Geochimica et Cosmochimica* **58(19)** 4147-4153.
- DENTEL S (1991) Coagulation control in water treatment. *CRC Critical Reviews in Environmental Control* **21** 41-135.
- DUAN J and GREGORY J (1996) Influence of soluble silica on coagulation by aluminium sulphate. *Colloids and Surfaces A: Physicochemical and Engineering Aspects* **107** 309-319.
- EVERETT DH (1988) *Basic Principles of Colloid Science*. London: Royal Society of Chemistry.
- FAIRTHORNE G, FORNASIERO D and RALSTON J (1997) Effect of oxidation on the collectorless flotation of chalcopyrite. *International Journal of Mineral Processing* **49(1-2)** 31-48.
- FORNASIERO D, EIJT V and RALSTON J (1992) An electrokinetic study of pyrite oxidation. *Colloids and Surfaces* **62(1-2)** 63-73.
- FRANKE J and MERSMANN A (1995) The influence of operational conditions on the precipitation process. *Chemical Engineering Science* **50(11)** 1737-1753.
- FULLSTON D, FORNASIERO D and RALSTON J (1999) Zeta potential study of the oxidation of sulfide minerals. *Colloids and Surfaces A: Physicochemical and Engineering Aspects* **146** 113-121.
- GARD R, SUN ZX and FORSLING W (1995) FT-IR and FT-Raman studies of colloidal ZnS. I. Acidic and alkaline sites at the ZnS water interface. *Journal of Colloid and Interface Science* **169(2)** 393-399.
- HAMMACK RW, DVORAK DH and EDENBORN HM (1993) *The use of biogenic hydrogen sulfide to selectively recover copper and zinc from severely contaminated mine drainage*. Warrendale, The Minerals, Metals and Materials Society, 631-639.
- HARMANDAS NG and KOUTSOUKOS PG (1996) The formation of iron (II) sulfides in aqueous solutions. *Journal of Crystal Growth* **3/4(167)** 719-724.

- HEALY TW and MOIGNARD MS (1976) *A review of electrokinetic studies of metal sulphides in flotation: A. M Gaudin Memorial Volume*. New York: American Institute of Mining, Metallurgical and Petroleum Engineers.
- HIEMSTRA T, VAN RIEMSDIJK WH and BOLT GH (1989) Multisite proton modeling at the solid/solution interface of (hydr)oxides: A new approach: I. Model description and evaluation of intrinsic reaction constants. *Journal of Colloid and Interface Science* **133** 91-104.
- HOVE M, VAN HILLE RP and LEWIS AE (2008) Mechanisms of formation of iron precipitates from ferrous solutions at high and low pH. *Chemical Engineering Science* **63** 1626-1635.
- HUDSON JB (1998) *Surface science: an introduction*. New York: John Wiley and Sons.
- HUISMAN JL, SCHOUTEN G and SCHULTZ C (2006) Biologically produced sulphide for purification of process streams, effluent treatment and recovery of metals in the metal and mining industry. *Hydrometallurgy* **83** 106-113.
- HUNTER RJ (1986). *Foundations of Colloid Science Volume 1*. New York: Oxford University Press.
- KARBANEE N, VAN HILLE RP and LEWIS AE (2008) Controlled nickel sulfide precipitation using gaseous hydrogen sulfide. *Industrial and Engineering Chemistry Research* **47** 1596-1602.
- KELEBEK S and SMITH GW (1989) Electrokinetic properties of a galena and chalcopyrite with the collectroless flotation. *Colloids and Surfaces* **40** 137-143.
- KOLTHOFF IM and MOLTZAU DR (1935) Induced precipitation and properties of metal sulfides *Chemical Reviews* **17** 293-325.
- LANGE AG, SKINNER WM and SMART RSC (1997) Fine:coarse particle interactions and aggregation in sphalerite flotation. *Minerals Engineering* **10(7)** 681-693.
- LEWIS AE (2010) Review of metal sulphide precipitation. *Hydrometallurgy* **104(2)** 222-234.
- LIU JC and HUANG CP (1992) Electrokinetic characteristics of some metal sulphide-water interfaces. *Langmuir* **8(7)** 1851-1856.
- MAROTO JA and DE LAS NIEVES FJ (1998) Influence of multiple light scattering on the estimation of homocoagulation and heterocoagulation rate constants by turbidity measurements. *Colloids and Surfaces A: Physicochemical and Engineering Aspects* **132(2-3)** 153-158.
- SANTHEEP K, MATHEW NP, RAJESH M and ICHIMURA U (2008) Preparation and characterisation of copper sulphide particles by photochemical method. *Materials Letters*, **62** 591-593.
- MEHTA SK, SANJAY K and GRADZIELSKI M (2011) Growth, stability, optical and photoluminescent properties of aqueous colloidal ZnS nanoparticles in relation to surfactant molecular structure. *Journal of Colloid and Interface Science* **360** 497-507.
- MERSMANN A (1999) Crystallisation and Precipitation. *Chemical Engineering and Processing: Process Intensification* **38(4-6)** 345-353.
- MERSMANN A (2001) *Crystallization Technology Handbook*. 2nd ed. New York: Marcel Dekker.
- MIRNEZAMI M, RESTREPO L and FINCH JA (2003) Aggregation of sphalerite: role of zinc ions. *Journal of Colloid Interface Science* **259** 36-42.
- MISHRA PK and DAS RP (1992) Kinetics of zinc and cobalt sulphide precipitation and its application in hydrometallurgical separation. *Hydrometallurgy* **3(28)** 373-379.
- MOIGNARD MS, JAMES RO and HEALY TW (1977) Adsorption of calcium at the zinc sulphide-water interface. *Australian Journal of Chemistry* **30(4)** 733-740.
- MOKONE TP, VAN HILLE RP and LEWIS AE (2012) Metal sulphides from wastewater: assessing the impact of supersaturation control strategies. *Water Research* **46(7)** 2088-2100.

- MOKONE T, VAN HILLE RP and LEWIS AE (2010) Effect of solution chemistry on particle characteristics during metal sulphide precipitation. *Journal of Colloid and Interface Science* **351** 10-18.
- MULLIN JW (2001). *Crystallization*. 4th ed. Oxford: Butterworth-Heinemann.
- MUSTER TH and PRESTIDGE CA (1995) Rheological investigations of sulphide mineral slurries. *Minerals Engineering* **8** 1541-1555.
- MUSTER TH, TOIKKA G, HAYES RA, PRESTIDGE CA and RALSTON J (1996) Interactions between zinc sulphide particles under flotation-related conditions. *Colloids and Surfaces A: Physicochemical and Engineering Aspects* **106(2-3)** 203-211.
- NEWEL AJH, SKINNER WM and BRADSHAW DJ (2007) Restoring the floatability of oxidised sulfides using sulfidisation. *International Journal of Mineral Processing* **84** 108-117.
- NICOLAU YF and MENARD JC (1992) An electrochemistry study of ZnS and CdS surface chemistry. *Journal of Colloid and Interface Science* **148** 552-570.
- NTULI F and LEWIS AE (2007) The influence of iron on the precipitation behaviour of nickel. *Chemical Engineering Science* **62** 3756-3766.
- OVERBEEK JTG (1977) Recent developments in the understanding of colloid stability. *Journal of Colloidal Interface Science* **2(58)** 408-422.
- PANKOW JF (1979) The dissolution rates and mechanisms of tetragonal ferrous sulphide (Mackinawite) in anoxic aqueous systems. *Doctor of Philosophy, California Institute of Technology*.
- PARKS G (1965) The isoelectric points of solid oxides, solid hydroxides and aqueous hydroxo complex systems. *Chemical Reviews* **65** 177-198.
- PEVERE A, GUIBAUD G, VAN HULLEBUSCH ED, BOUGHZALA W and LENS PNL (2007) Effect of Na<sup>+</sup> and Ca<sup>2+</sup> on the aggregation properties of sieved granular sludge. *Colloids and Surfaces* **306** 142-149.
- RANDOLPH AD and LARSON MA (1988) *Theory of particulate processes*. 2nd ed. London: Academic Press.
- REERINK H and OVERBEEK JG (1954) The rate of coagulation as a measure of the stability of silver iodide sols. *Discussions of the Faraday Society* **18** 74-84.
- RICKARD D (1995) Kinetics of FeS precipitation: Part 1. Competing reaction mechanisms. *Geochimica et Cosmochimica Acta* **21(59)** 4367-4379.
- RICKARD D (2006) The solubility of FeS. *Geochimica et Cosmochimica Acta* **70(23)** 5779-5789.
- SAAD RF (1998) Selected heavy metal and organic removal from waste water by precipitation and ozonation processes. *Master of Applied Science, University of Ottawa*.
- SAMPAIO RMM, TIMMERS RA, KOCKS N, ANDRÉ V, DUARTE MT, VAN HULLEBUSCH ED, FARGES F and LENS PNL (2010) Zn-Ni sulfide selective precipitation: The role of supersaturation. *Separation and Purification Technology* **74** 108-118.
- SCHLAUCH RM (1978) *Colloid free precipitation of heavy metal sulfides*. USA, Patent No. 4102784.
- SENANAYAKE G (2009) A review of chloride assisted copper sulphide leaching by oxygenated sulphuric acid and mechanistic consideration. *Hydrometallurgy* **98** 21-32.
- SHAW DJ (1970) *Introduction to colloid and surface chemistry*. London: Butterworths.
- SÖHNEL O and GARSIDE J (1992) *Precipitation: basic principles and industrial applications*. Oxford: Butterworth-Heinemann.
- STUMM W (1992) *Chemistry of the solid-water interface: processes at the mineral-water and particle-water interface in natural systems*. New York: John Wiley and Sons Inc.

- TATY COSTODES VC and LEWIS AE (2006) Reactive crystallization of nickel-hydroxy-carbonate in a fluidised bed reactor: 1 Fines production and column design. *Chemical Engineering Science* **61** 1377-1385.
- VAN HILLE RP, DUNCAN J and LEWIS AE (2005) Heavy metal precipitation by sulphide and bicarbonate: Evaluating methods to predict anaerobic digester overflow performance. In: *Proceedings of the International Mine Water Association Symposium*, University of Newcastle, Newcastle upon Tyne, UK, ISBN 0-9543827-3-0, 141-150.
- VEEKEN AHM, AKOTO L, HULSHOFF POL LW and WEIJMA J (2003) Control of sulfide concentration for optimal zinc removal by sulfide precipitation in a continuously stirred tank reactor. *Water Research* **37** 3709-3717.
- VERGOUW JM, DIFEO A, XU Z and FINCH JA (1998) An agglomeration study of sulphide minerals using zeta-potential and settling rate. Part I: Pyrite and galena. *Minerals Engineering* **11(2)** 159-169.
- WILLIAMS R and LABIB ME (1985) Zinc sulphide chemistry: An electrokinetic study. *Journal of Colloid and Surface Science* **106** 252-254.
- YANG-XIN Y, JIANZHONG W and GUANG-HUA G (2004) Density-functional theory of spherical electric double layers and zeta potentials of colloidal particles in restricted-primitive-model electrolyte solutions. *Journal of Chemical Physics* **120(15)** 7223-7233.
- ZHANG Q, XU Z and FINCH JA (1995) Surface ionization and complexation at the sphalerite/water interface. *Journal of Colloid and Interface Science* **169(2)** 414-421.